

Pacific Gas & Electric

DEVELOPMENT OF GROUNDWATER FLOW AND SOLUTE TRANSPORT MODELS

Pacific Gas & Electric

Topock Compressor Station

Needles, California

February 2016

**DEVELOPMENT
OF GROUNDWATER
FLOW AND SOLUTE
TRANSPORT MODELS**

**TOPOCK COMPRESSOR STATION
NEEDLES, CALIFORNIA**



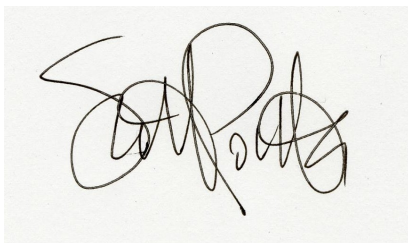
Jenifer Wahlberg
Engineer 2

Prepared for:
Pacific Gas and Electric Company
PG&E Topock Compressor Station
Needles, California



Jonathan Roller
Senior Hydrogeologist

Prepared by:
Arcadis U.S., Inc.
10 Friends Lane
Suite 200
Newtown
Pennsylvania 18940
Tel 267 685 1800
Fax 267 685 1801



Scott Potter
Chief Hydrogeologist

Our Ref.:
RC000753.0031
Date:
February 29, 2016

VERSION CONTROL

Issue	Revision No	Date Issued	Page No	Description	Reviewed by

CONTENTS

Acronyms and Abbreviations.....	vi
Executive Summary.....	1
1 Introduction and Objectives	3
1.1 General	3
1.2 Site Location and Description	3
1.3 Report Objectives and Organization.....	3
2 Conceptual Site Model.....	4
2.1 Site Geology and Hydrogeology	4
2.2 Geology.....	4
2.2.1 Hydrostratigraphic Units	5
2.2.1.1 Fluvial (River) Deposits.....	6
2.2.1.2 Quaternary Alluvium (Qoa).....	6
2.2.1.3 Bouse Formation	6
2.2.1.4 Tertiary Alluvium	6
2.2.1.5 Basal Alluvium	6
2.2.1.6 Bedrock.....	7
2.3 Hydrogeology.....	7
2.4 Site Geochemistry.....	9
3 Groundwater Flow Model Development	10
3.1 Model Code Selection and Description	10
3.2 Model Domain and Grid	11
3.3 Boundary Conditions	11
3.4 Hydraulic Parameters	13
3.4.1 Hydraulic Conductivity	13
3.4.2 Evapotranspiration.....	13
3.4.3 Recharge	14
3.5 Groundwater Flow Model Calibration	14
3.5.1 Steady State Calibration.....	14
3.5.1.1 Pre IM-3 Conditions	18

DEVELOPMENT OF GROUNDWATER FLOW AND SOLUTE TRANSPORT MODELS

3.5.1.2	Active IM-3 Conditions	19
3.5.2	Transient Calibration	20
3.6	Simulated Groundwater Flow	21
3.7	Sensitivity Analyses	22
3.7.1	Hydraulic Conductivity	22
3.7.2	Recharge	Error! Bookmark not defined.
3.7.3	Riverbed Conductance	23
3.7.4	Evapotranspiration.....	23
3.7.5	Leakance	24
4	Solute Transport Model Development	25
4.1	Code Selection.....	25
4.2	Solute Transport Parameters.....	26
4.2.1	Porosity.....	26
4.2.2	Mass Transfer Coefficient	27
4.2.3	Chromium Adsorption.....	27
4.2.4	Chromium Reduction.....	28
4.2.5	Initial Hexavalent Chromium Distribution	28
4.2.6	Byproduct Generation	28
4.2.7	Byproduct Adsorption and Precipitation	29
4.3	Parameter Assessment	31
4.4	Remediation Design.....	31
4.5	Pathline Analysis.....	31
5	Solute Transport Model Results.....	32
5.1	Hexavalent Chromium	32
5.2	Manganese	33
5.3	Arsenic	33
6	Uncertainty	34
7	Model Update Procedure	34
7.1	Well Installation and Testing.....	35
7.2	Remedy Start-up and Operation.....	37
8	Summary and Conclusions	38

9 References..... 39

TABLES

Table 2.2-1 Hydrostratigraphic Units
 Table 3.2-1 Model Vertical Structure
 Table 3.5-1 Pre IM-3 Water Level Targets and Residuals
 Table 3.5-2 Active IM-3 Water Level Targets and Residuals
 Table 3.5-3 Pre IM-3 Water Balance
 Table 3.5-4 Active IM-3 Water Balance
 Table 3.5-5 Hydrostratigraphic Unit Storativity Values
 Table 3.7-1 Hydraulic Conductivity Sensitivity Analysis
 Table 3.7-2 Riverbed Conductance Sensitivity Analysis
 Table 3.7-3 Evapotranspiration Sensitivity Analysis
 Table 3.7-4 Global Leakance Sensitivity Analysis
 Table 3.7-5 Layerwise Leakance Sensitivity Analysis
 Table 4.2-1 Byproduct Generation Terms Used in Fate and Transport Model
 Table 4.2-2 Byproduct Sorption Terms Used in Fate and Transport Model

FIGURES

Figure 1-1 Site Location
 Figure 3.2-1 Finite Difference Grid
 Figure 3.2-2 Conceptual Final Groundwater Remedy Cross-Section Locations
 Figure 3.2-3 Conceptual Final Groundwater Remedy Cross-Section A-A'
 Figure 3.2-4 Conceptual Final Groundwater Remedy Cross-Section B-B'
 Figure 3.2-5 Conceptual Final Groundwater Remedy Cross-Section C-C'
 Figure 3.2-6 Conceptual Final Groundwater Remedy Cross-Section D-D'
 Figure 3.2-7 Conceptual Final Groundwater Remedy Cross-Section E-E'
 Figure 3.2-8 Conceptual Final Groundwater Remedy Cross-Section F-F'
 Figure 3.3-1 Boundary Conditions

DEVELOPMENT OF GROUNDWATER FLOW AND SOLUTE TRANSPORT MODELS

- Figure 3.4-1 Hydrostratigraphic Units Model Layers 1-5
- Figure 3.4-2 Hydrostratigraphic Units Model Layers 6-10
- Figure 3.4-3 Hydraulic Conductivity Zones Model Layer 1-5
- Figure 3.4-4 Hydraulic Conductivity Zones Model Layers 6-10
- Figure 3.4-5 Evapotranspiration Zones
- Figure 3.5-1 Simulated vs. Observed Water Levels- Pre-IM-3 Conditions
- Figure 3.5-2 Simulated vs. Observed Water Levels – Active IM-3 Conditions
- Figure 3.5-3 Simulated vs. Observed Water Levels – Transient Calibration
- Figure 3.5-4 Floodplain Transient Hydrographs
- Figure 3.5-5 Uplands Transient Hydrographs
- Figure 3.6-1 Regional Simulated Water Level Model Layer 1
- Figure 3.6-2 Site Simulated Water Level Model Layer 1
- Figure 3.7-1 Sensitivity Analysis
- Figure 3.7-2 Sensitivity Analysis Leakance by Layer
- Figure 4.2-1 Initial Hexavalent Chromium Distribution Model Layers 1-5 2013
- Figure 4.2-2 Initial Hexavalent Chromium Distribution Model Layers 1-5 2015
- Figure 4.4-1 Remediation Design Well Locations
- Figure 4.4-1 Simulated Subsurface Groundwater Flow and Pathlines Model Layer 1 – NTH IRZ ON
- Figure 4.4-2 Simulated Subsurface Groundwater Flow and Pathlines Model Layer 1 – NTH IRZ OFF
- Figure 4.4-3 Simulated Subsurface Groundwater Flow and Pathlines Model Layer 2 – NTH IRZ ON
- Figure 4.4-4 Simulated Subsurface Groundwater Flow and Pathlines Model Layer 2 – NTH IRZ OFF
- Figure 4.4-5 Simulated Subsurface Groundwater Flow and Pathlines Model Layer 3 – NTH IRZ ON
- Figure 4.4-6 Simulated Subsurface Groundwater Flow and Pathlines Model Layer 3 – NTH IRZ OFF
- Figure 4.4-7 Simulated Subsurface Groundwater Flow and Pathlines Model Layer 4 – NTH IRZ ON
- Figure 4.4-8 Simulated Subsurface Groundwater Flow and Pathlines Model Layer 4 – NTH IRZ OFF
- Figure 4.4-9 Simulated Subsurface Groundwater Flow and Pathlines Model Layer 5 – NTH IRZ ON
- Figure 4.4-10 Simulated Subsurface Groundwater Flow and Pathlines Model Layer 5 – NTH IRZ OFF
- Figure 5.1-1 Simulated Hexavalent Chromium Transport Results in Model Layer 1 with 2013 Initialized Plumes
- Figure 5.1-2 Simulated Hexavalent Chromium Transport Results in Model Layer 2 with 2013 Initialized Plumes

DEVELOPMENT OF GROUNDWATER FLOW AND SOLUTE TRANSPORT MODELS

- Figure 5.1-3 Simulated Hexavalent Chromium Transport Results in Model Layer 3 with 2013 Initialized Plumes
- Figure 5.1-4 Simulated Hexavalent Chromium Transport Results in Model Layer 4 with 2013 Initialized Plumes
- Figure 5.1-5 Simulated Hexavalent Chromium Transport Results in Model Layer 5 with 2013 Initialized Plumes
- Figure 5.1-6 Simulated Hexavalent Chromium Transport Results in Model Layer 1 with 2015 Initialized Plumes
- Figure 5.1-7 Simulated Hexavalent Chromium Transport Results in Model Layer 2 with 2015 Initialized Plumes
- Figure 5.1-8 Simulated Hexavalent Chromium Transport Results in Model Layer 3 with 2015 Initialized Plumes
- Figure 5.1-9 Simulated Hexavalent Chromium Transport Results in Model Layer 4 with 2015 Initialized Plumes
- Figure 5.1-10 Simulated Hexavalent Chromium Transport Results in Model Layer 5 with 2015 Initialized Plumes
- Figure 5.2-1 Simulated Manganese Transport Results
- Figure 5.3-1 Simulated Arsenic Transport Results

APPENDICES

- Appendix A Transient Calibration Data

ACRONYMS AND ABBREVIATIONS

bgs	below ground surface
CMS/FS	Corrective Measures Study/Feasibility Study
Cr(III)	trivalent chromium
Cr(VI)	hexavalent chromium
CSM	conceptual site model
ft ²	square feet
ft ³	cubic feet
ft/ft	foot per foot
Floodplain ISPT Final Completion Report	Floodplain Reductive Zone In-Situ Pilot Test Final Completion Report
gpm	gallons per minute
IM	interim measure
IRL	Inner Recirculation Loop
IRZ	in-site reactive zone
ISPT	in-situ pilot test
kg/day	kilograms per day
L/kg	liters per kilogram
m ² /g	square meters per gram
mg	milligram
mg/kg	milligrams per kilogram
mg/L	milligrams per liter
msl	mean sea level
MTC	mass transfer coefficient
mV	millivolt
ng/L	nanograms per liter
NTH	National Trails Highway
ORP	oxidation-reduction potential
PG&E	Pacific Gas and Electric Company
redox	oxidation-reduction

DEVELOPMENT OF GROUNDWATER FLOW AND SOLUTE TRANSPORT MODELS

SCM	surface complexation model
TCS	Topock Compressor Station
TDS	total dissolved solid
TOC	total organic carbon
µg/L	micrograms per liter
USEPA	United States Environmental Protection Agency

EXECUTIVE SUMMARY

Pacific Gas and Electric Company (PG&E) is implementing the selected groundwater remedy for chromium in groundwater at the PG&E Topock Compressor Station (TCS, or the Compressor Station) in San Bernardino County, California. Remedial activities at the Topock site are being performed in conformance with the requirements of the Resource Conservation and Recovery Act (RCRA) Corrective Action pursuant to a Corrective Action Consent Agreement (CACA) entered into by PG&E and the California Department of Toxic Substances Control (DTSC) in 1996. In addition, PG&E and the United States executed a Remedial Design/Remedial Action Consent Decree (CD), on behalf of the Department of the Interior (DOI), under the Comprehensive Environmental Response, Compensation, and Liability Act (CERCLA) in 2012, which was approved by the U.S. District Court for the Central District of California in November 2013. The TCS is approximately 1,500 feet west of the Colorado River and ½ mile west of Topock, Arizona. This document, Development of Groundwater Flow and Solute Transport documents the updates made to the groundwater flow and solute transport models that were constructed for the Site as documented in Appendix B of the 100% Basis of Design (Arcadis, 2015). These updates were conducted in compliance with the DOI and DTSC Final Design Directives dated October 19, 2016. The groundwater flow and solute transport model were developed to evaluate the subsurface flow conditions; including the fate and transport of Cr(VI), manganese, and arsenic.

The major components of the updated groundwater flow and solute transport model are presented in this document. Updates to the regional groundwater flow model include lithologic and hydraulic data that had become available since the original calibration (as described in the 30%, 60%, 90%, and 100% basis of design documents), expansion of the regional flow model domain, and conversion of the regional flow model from MicroFEM to MODFLOW in order to directly conduct solute transport analyses without having to extract a submodel. Geochemical modeling (batch and one-dimensional transport simulations) conducted for the 100% basis of design document were utilized to evaluate the anticipated behavior of reactive species during remedy implementation, including TOC, Cr(VI), and byproducts as a function of groundwater geochemistry and aquifer properties. These focused geochemical evaluations were conducted to characterize known geochemical reactions that will occur and to aid in the estimation of parameters used in the site-wide solute transport model. The geochemical modeling was also conducted to test the validity of the site-wide solute transport model in describing Cr(VI) reduction and byproduct dynamics. Solute transport modeling was performed to evaluate the migration and fate of Cr(VI) detected in the groundwater, the fate and transport of select potential IRZ byproducts (manganese and arsenic), and the fate and transport of arsenic associated with the freshwater source injected into the uplands. The solute transport model used the flow results from the calibrated groundwater flow model to simulate solute transport under average flow conditions. Finally, a detailed sensitivity analysis was conducted to evaluate the effects of varying hydraulic parameters on the calibration of the groundwater flow model.

Based on this update of the groundwater flow model and associated solute transport modeling, the solute transport model results indicates that the planned remedy will be effective in remediating the current Cr(VI) plume distribution while minimizing the potential adverse impacts from byproduct generation. This solute transport model can be utilized as a tool to evaluate potential remedial options and supplements monitoring of the implemented remedial system to measure its effectiveness. During installation and implementation of the remedial system, the additional hydrogeologic and groundwater quality data

DEVELOPMENT OF GROUNDWATER FLOW AND SOLUTE TRANSPORT MODELS

generated can be utilized to update the groundwater flow and transport models to improve their effectiveness as tools for further understanding site conditions and optimizing the remedy performance.

1 INTRODUCTION AND OBJECTIVES

1.1 General

This report has been prepared for Pacific Gas and Electric Company (PG&E) to present a conceptual Site model (CSM), a calibrated groundwater flow model, sensitivity analyses, and a solute transport model for the PG&E Topock Compressor Station (TCS, or the Compressor Station) in San Bernardino County, California (Figure 1-1).

1.2 Site Location and Description

Remedial activities at the Topock Site are being performed in conformance with the requirements of the Resource Conservation and Recovery Act (RCRA) Corrective Action pursuant to a Corrective Action Consent Agreement (CACA) entered into by PG&E and the California Department of Toxic Substances Control (DTSC) in 1996. In addition, PG&E and the United States executed a Remedial Design/Remedial Action Consent Decree (CD), on behalf of the Department of the Interior (DOI), under the Comprehensive Environmental Response, Compensation, and Liability Act (CERCLA) in 2012, which was approved by the U.S. District Court for the Central District of California in November 2013. The TCS is approximately 1,500 feet west of the Colorado River and ½ mile west of Topock, Arizona.

1.3 Report Objectives and Organization

The objectives of this modeling study were to develop a groundwater flow and solute transport model for use as follows:

- Expand the domain of the regional groundwater flow model and convert the regional groundwater flow model from MicroFEM to MODFLOW;
- Restructure the groundwater flow model to more accurately simulate the interaction between the alluvial aquifer and bedrock with respect to solute transport;
- Identify the major hydrostratigraphic units and represent these units with distinct hydraulic conductivity zones;
- Conduct detailed steady state and transient groundwater flow model calibrations to refine hydraulic parameter values;
- Conduct a sensitivity analysis to evaluate the hydraulic parameters utilized in the groundwater flow model; and
- Evaluate the remedial design from the 100% basis of design with the updated groundwater flow and solute transport model with respect to transport of hexavalent chromium, byproduct manganese, byproduct arsenic, and arsenic associated with freshwater injection in the uplands.

This document describes the results of four major components of the modeling study at the Site:

- updates to and the development of the groundwater flow model
- calibration of the groundwater flow model

DEVELOPMENT OF GROUNDWATER FLOW AND SOLUTE TRANSPORT MODELS

- development of the solute transport model
- remediation system analysis

The above components are presented in the following sections of the report:

- Section 2 – Conceptual Site Model (CSM)
- Section 3 – Groundwater Flow Model Development
- Section 4 – Solute Transport Model Development
- Section 5 – Solute Transport Model Results
- Section 6 – Model Uncertainty
- Section 7 – Model Update Procedure

2 CONCEPTUAL SITE MODEL

A CSM is a description of the key components and processes underlying a physical system and provides a framework for the Site. In the case of the Topock Site, the CSM describes the hydrogeology and associated geochemistry and utilizes a basic framework of Source-Pathway-Receptor to describe how contaminants enter an environmental system (source), migrate within it (pathway), and eventually reach their ultimate receptors (receptor). The CSM serves as the basis for quantitative modeling of groundwater flow and contaminant fate and transport that simulates the operation of the remediation system; and it provides the foundational framework for the design and operation of the remediation system

2.1 Site Geology and Hydrogeology

The conceptual model for groundwater flow herein is a narrative description of the principal components of the groundwater flow system developed from regional, local, and Site-specific data. The primary components of the groundwater flow system include: (1) areal extent, configuration, and types of aquifers and aquitards; (2) hydraulic properties of aquifers and aquitards; (3) natural groundwater recharge and discharge zones; (4) anthropogenic influence on groundwater (sources and sinks); and (5) areal and vertical distribution of groundwater hydraulic head potential. These aquifer system components serve as the framework for the construction of the numerical groundwater flow model (described in Section 3). Sections 2.2 and 2.3, below, describe the regional and Site hydrogeology, respectively.

2.2 Geology

The Site is situated in a basin-and-range geologic environment in the Mohave Valley. The Colorado River is the main source of water to this groundwater basin, but at the southern end where the Site is located, groundwater is also fed by a relatively modest amount of local recharge from mountain runoff. The most prominent geologic structural feature in the area of the Site is a Miocene-age, low-angle normal fault (referred to as a detachment fault) that forms the northern boundary of the Chemehuevi Mountains that

are located to the southeast of the Site. The surface expression of the Chemehuevi detachment fault is evident as a pronounced northeast-southwest linear feature that can be traced along the northern boundary of the Chemehuevi Mountains, terminating at the abrupt bend in the Colorado River east of the TCS. The exposed Chemehuevi Mountains are Precambrian- and Mesozoic-age metamorphic and igneous rocks formed by tectonic uplift along the present-day trace of the Chemehuevi detachment fault.

Sedimentary deposits in the area are comprised of Pliocene lacustrine deposits, Tertiary- and Quaternary-age to recent alluvial fan deposits, and fluvial deposits of the Colorado River. The younger Colorado River fluvial deposits occur at the Site within the saturated zone underlying the floodplain, the present river channel, and the associated marsh area (Metzger and Loeltz 1973; Howard et al. 1997).

2.2.1 Hydrostratigraphic Units

There are ten characteristic hydrostratigraphic units (HSUs) in the region (Table 2.2-1) (CH2M Hill, 2006b).

Table 2.2--1 Hydrostratigraphic Units

Index	Stratigraphic Age	Site HSU	Deposit	Description	Characteristics
1	Holocene	Qr3	Fluvial	Upper Fluvial Sand and Silt	Unconsolidated sand and silty sand (no gravel), massive bedded, very well sorted; contains fine grained organic matter
2		Qr2	Fluvial	Middle Fluvial Deposits	Interbedded unconsolidated sand, clay, and minor gravelly sand; clay/silt lenses exhibit both brown and gray (reduced) appearance
3		Qr1	Fluvial	Lower Fluvial Deposits	Unconsolidated sandy gravel and gravelly sand with minor silty gravel (gravel content greater than 15%); subrounded to very well-rounded pebbles and cobbles from distant sources and fluvial deposits
4		Qr0	Fluvial	Colorado River Channel Fill	Fluvial channel fill sediments that occur below elevation 360 ft msl (deepest river deposits encountered in floodplain borings). Per Caltrans I-40 bridge borings includes moderately consolidated to dense, fine to coarse sand and sandy gravel
5	Pleistocene	Qoa	Alluvium	Older Quaternary Alluvium	Unconsolidated sandy gravel and silty/clayey gravel (alluvial fan deposits). Comprises moderately-dissected alluvial terraces' terrace/wash slopes are moderate angle (i.e., 45 degrees)
6	Pliocene	Tb	Alluvium	Bouse Formation	Pre-Colorado River lacustrine and deltaic deposits (well bedded, moderately indurated, green clay, siliceous claystone, sandstone, and basal marl)
7	Pliocene to Late Miocene	Toa2	Alluvium	Tertiary Alluvium - Upper	Moderately consolidated sandy gravel, gravelly sand, and silty/clayey gravel (oldest alluvial fan deposits). Comprises deeply-dissected alluvial terraces; terrace canyon walls are vertical/steep (Subdivision of Toa2 and Toa1 based on contrasts in hydraulic conductivity observed in TW-1, TW-2D, and IW-1).
8		Toa1	Alluvium	Tertiary Alluvium - Lower	

DEVELOPMENT OF GROUNDWATER FLOW AND SOLUTE TRANSPORT MODELS

9	Late Miocene	Toa0	Alluvium	Basal Alluvium	Moderately consolidated silty sand, clayey/silty gravel, and minor gravelly sand. Consists of 100% reddish detritus of Miocene conglomerate in floodplain area. In other areas, Toa0 is well-consolidated alluvium, lacks reddish-color, and exhibits high-induction geophysical log response
10	Middle Miocene Pre-tertiary	Bedrock	Bedrock	Miocene Conglomerate Metamorphic/Igneous Bedrock	Consolidated conglomerate, sandstone, metadiorite, gneiss, and granitic bedrock

2.2.1.1 Fluvial (River) Deposits

The Colorado River deposits (or fluvial deposits) lie from the Topock floodplain eastward to the edge of Topock Bay and Topock Marsh. The thickness of the fluvial deposits ranges from near zero to approximately 250 feet observed in the river seismic survey conducted by the USGS (Peter Martin, Technical Work Group meeting communications 2004). Four HSUs comprise the fluvial deposits: Qr3, Qr2, Qr1, and Qr0 (from the youngest to the oldest).

2.2.1.2 Quaternary Alluvium (Qoa)

The quaternary alluvial deposits overlie the Bouse Formation, where the Bouse Formation is present. Where the Bouse Formation is not present, the Quaternary and Tertiary Alluvial deposits are virtually indistinguishable in site borings. However, in outcrops, the difference between the Quaternary and Tertiary Alluvial deposits is the Quaternary Alluvium has a moderate angle (around 45 degrees).

2.2.1.3 Bouse Formation

The Bouse Formation is located in the western portion of the model domain and consists of interbedded clay, claystone, and sandstone. This formation represents a lacustrine deposit left by a large portion of the Mohave Valley (Howard et al, 1997). However, much of the Bouse Formation was eroded away during the Pleistocene and Holocene Epochs. In Site boring logs, no saturated portion of the Bouse Formation has been encountered.

2.2.1.4 Tertiary Alluvium

The tertiary alluvium consists of sandy gravel and silty/clayey gravel. The tertiary alluvium was divided into lower and upper units based on hydraulic permeability contrasts observed in well testing and variations in geophysical log responses.

2.2.1.5 Basal Alluvium

The basal alluvium has previously been described as either the “Basal Saline Unit” or “reworked Miocene Conglomerate” (CH2M Hill, 2006b). Geophysical induction logging indicates that there is much higher salinity and finer grained material in the basal alluvium than in most of the tertiary alluvium.

2.2.1.6 Bedrock

The bedrock at the Site consists of Pre-Tertiary igneous and metamorphic rock and the Miocene conglomerate. In general, both bedrock units are considered to produce very little water and to be locally fractured (CH2M Hill, 2006b). There is an upward hydraulic gradient between the bedrock units and the alluvial units.

2.3 Hydrogeology

The Site is located at the southern (downstream) end of the Mohave Valley groundwater basin. On a regional scale, groundwater in the northern and central area of the valley is recharged primarily by the Colorado River, while under natural conditions net groundwater discharges occur in the southern area, above where the alluvial aquifer thins near the entrance to Topock Gorge. Regional groundwater flow occurs from north to south, following the direction of flow in the Colorado River. The groundwater directly beneath the Site is derived mostly from the relatively small recharge from the nearby mountains. Under natural conditions, groundwater flows from west/southwest to east/northeast across the Site.

The Colorado River is 1,500 feet east of the TCS with a mean elevation of approximately 450 feet above mean sea level (msl). The TCS is at an elevation of approximately 600 feet above msl on an extensive alluvial terrace that is locally incised by erosional channels formed by surface runoff. Thus, the surface slope is generally toward the river from areas west of the river. Bat Cave Wash, a large north-south erosional channel adjacent to the TCS, only has surface-water flow after large precipitation events. The stretch of the Colorado River east of the Site is 600 to 700 feet wide. Flow in the river fluctuates daily and seasonally due to upstream-regulated water releases by the Bureau of Reclamation at Davis Dam on Lake Mohave. Measured flows range from 4,000 to 25,000 cubic feet per second, and river levels fluctuate between 2 and 3 feet within a single day, depending on the time of year.

Groundwater occurs in the Tertiary-age and younger alluvial fan and fluvial deposits. These deposits are unconsolidated alluvial and fluvial deposits and are underlain by the Miocene-age conglomerate, which is consolidated, and pre-Tertiary-age metamorphic and igneous rocks. Both the conglomerate and igneous/metamorphic units are considered to be bedrock at the Site. The bedrock typically has lower permeability; therefore groundwater movement occurs primarily in the overlying unconsolidated deposits. There is no evidence to indicate any sizable potential for development of groundwater in the bedrock, although locally, small yields may be developed from fractures (Metzger and Loeltz 1973).

This conceptual framework for the bedrock system is supported by recent investigation work in the East Ravine and TCS areas. Of the 17 boreholes that have been drilled into appreciable depths within the bedrock in the East Ravine and TCS areas, only two boreholes, MW-57-185 and MW-70BR-225 (which are both located in close proximity to the approximate bedrock/alluvial aquifer contact at elevation 455 feet above msl), have yielded enough groundwater to sustain pumping for relatively low-volume hydraulic testing. During the test at MW-57-185 (pumped at approximately 3 gallons per minute [gpm] for 7 hours), approximately 78 feet of drawdown was observed within the pumping well, while drawdown of more than 0.05 foot was observed in only one of the seven observation wells (MW-58BR, 0.07 foot). Drawdown in the other six bedrock observation wells was less than 0.05 foot. During the test at MW-70BR-225 (pumped at approximately 9 gpm for 12 hours), approximately 34 feet of drawdown was observed in the pumping well, while drawdown of more than 0.05 foot was observed in only one of the 10 bedrock

DEVELOPMENT OF GROUNDWATER FLOW AND SOLUTE TRANSPORT MODELS

observation wells (MW-58BR, 0.18 foot).¹ Drawdown in the other nine bedrock observation wells was less than 0.05 foot. During both tests, the yield from the bedrock was insufficient to induce measurable drawdown in wells screened within the unconsolidated alluvial sediments. All other Site bedrock monitoring wells yield very small quantities of groundwater, with several that have become dewatered during routine sampling. These data are consistent with the regional hydrogeology.

The alluvial aquifer within the groundwater basin and beneath the Site consists of: (1) unconsolidated alluvial sands and gravels shed from local mountain ranges that ring the valley and (2) unconsolidated fluvial material deposited by the Colorado River. Groundwater occurs under unconfined to semi-confined conditions within the alluvial and fluvial sediments beneath most of the Site. The alluvial sediments consist primarily of silty sand and gravel deposits (with a relatively minor amount of clay) interfingering with more permeable sand and gravel deposits. The alluvial deposits exhibit an expected considerable variability in hydraulic conductivity between fine- and coarse-grained sequences. The fluvial sediments similarly consist of interbedded sand, sandy gravel, and silt/clay.

The water table in the alluvial aquifer is nearly flat and typically equilibrates to an elevation within 3 feet of the river level. Due to the variable topography, the depth to groundwater ranges from as shallow as 5 feet below ground surface (bgs) in the floodplain near the river to approximately 170 feet bgs in the upland alluvial terrace areas. The saturated thickness of the alluvial aquifer is approximately 100 feet in the floodplain and thins to the south, pinching out along locations where the Miocene Conglomerate and igneous/metamorphic rocks outcrop. In the western and northern portions of the Site, where the depth to bedrock increases, the saturated thickness of the alluvial aquifer is over 200 feet.

Several other important hydrogeologic features of the Site are summarized below:

- Under ambient conditions in the vicinity of the Site, the Colorado River recharges groundwater during the higher-flow stages in the spring and summer months, and discharges groundwater to the river during the months of lower river stages in fall and winter. Since 2004, the Interim Measure (IM) groundwater extraction and treatment system has maintained a consistent, year-round landward gradient in the area where the plume is present in the floodplain (i.e., maintains a situation where the river discharges to groundwater). The hydraulic gradient imposed by IM-3 pumping is measured in three pairs of monitoring wells. Over the period from August 2007 through December 2011, the average landward gradient in these three well pairs was approximately 0.005 foot per foot (ft/ft).
- Under natural conditions, groundwater flow is generally from the west-southwest to east-northeast across the Site. Localized areas of northward flow likely occur along the mountain front to the south of the TCS. Hydraulic gradients are very small due to the limited recharge, with a typical value of 0.0005 ft/ft in the alluvial area. Under average conditions, groundwater velocity in the alluvial aquifer ranges from approximately 25 to 46 feet per year, according to numerical model estimates. The

¹ This excludes drawdown observed in the water-table well adjacent to pumping well (MW-70-105), which showed a dewatering trend during the test.

vertical component of the hydraulic gradient is upward between bedrock and the overlying alluvial aquifer and typically, but not universally, upward within the alluvial aquifer.

Groundwater level monitoring in the East Ravine area indicates that the groundwater in fractured bedrock is in hydraulic communication with the alluvial aquifer and equilibrates to an approximate elevation similar to the water table in the alluvial aquifer. Compared to the alluvial aquifer, the fractured rock permeabilities are very low, based on well tests in this area.

The unconsolidated aquifer consists of alluvial sands and gravels derived primarily from the metadiorite and gneissic rocks from the mountains that ring the groundwater basin, as well as fluvial material deposited by the Colorado River over time. These materials govern the observed groundwater geochemistry at the Site. A detailed description of the general groundwater quality and geochemistry at the Site can be found in the RCRA Facility Investigation/Remedial Investigation Report (CH2M HILL 2009a); a brief summary is provided herein.

2.4 Site Geochemistry

The groundwater at the Site is a sodium chloride-dominated type with highly variable total dissolved solid (TDS), varying from less than 1,000 milligrams per liter (mg/L) to greater than 10,000 mg/L. The most frequent values range between approximately 4,000 (33rd percentile) to 7,000 mg/L (66th percentile) and the median value is approximately 5,000 mg/L based on the most recent Site-wide TDS data collected through December 31, 2013. In general, higher TDS levels are encountered in deeper alluvial wells and a few shallow fluvial wells near the alluvium-bedrock interface. Groundwater TDS generally increases with depth throughout the Site. There are 30 Site well clusters that show this trend, and the average TDS increase between shallow and deep zones in these clusters is approximately 6,600 mg/L, with only seven clusters showing a difference greater than 10,000 mg/L. Groundwater density is proportional to TDS, and significant differences in density over the saturated thickness can cause non-uniform injected flow (Ward et al., 2008). However, the TDS ranges in Topock Site profiles are not expected to be large enough to cause issues in the remedy application.

The groundwater pH generally ranges between 7 and 8.5 and alkalinity is typically between 30 and 300 mg/L as calcium carbonate (although values as high as 800 to 1,000 mg/L have been measured in some areas).

Although the alluvial fan and fluvial deposits are of different origin, groundwater flows from the alluvial fan sediments into the fluvial zone sediments; therefore, the groundwater geochemistry in the fluvial zone is strongly influenced by alluvial groundwater geochemistry. One important difference between alluvial and fluvial zones is the presence of a reducing environment in shallow and mid-depth fluvial zones located within the Colorado River floodplain, caused by organic material deposited with the sediment. This reducing zone is characterized by generally lower levels of oxidation-reduction potential (ORP). Alluvial fan zones at the Site tend to exhibit ORP levels in the 0 to 300 millivolt (mV) range, while groundwater in the floodplain “reducing rind” fluvial aquifer can exhibit values in the -220 to -90 mV range, sufficiently reducing for Cr(VI) reduction. This reducing rind exists in the shallow portion of the fluvial aquifer, extending 200 to 500 feet away from the riverbank, generally getting thicker (i.e., penetrating deeper) with proximity to the river. The reducing rind correlates with decreases in nitrate concentrations, which is

detected across the Site at concentrations ranging up to 20 mg/L NO₃-N in the alluvial aquifer, but is non-detect in most areas of the reducing rind. Higher dissolved concentrations of manganese, iron, and organic carbon in the floodplain are also consistent with the more strongly reducing environment resulting from organic deposition (greater than 5 mg/L manganese and greater than 10 mg/L iron in some monitoring wells). These higher concentrations of manganese and iron are due to the reductive dissolution of naturally occurring iron and manganese oxides present within the floodplain. Hexavalent chromium is not stable under these conditions and is reduced to trivalent chromium, which is removed from solution as a stable hydroxide precipitate.

The boundary of this reducing rind is defined herein using multiple geochemical oxidation-reduction (redox) indicators, including nitrate, dissolved iron, organic carbon, and ORP. Generally, ORP is not as reliable an indicator of reducing conditions as the direct measurement of the concentration of other redox indicators, most notably nitrate and dissolved iron. The determination of ORP is based upon field electrode measurements, and these are more likely to be subject to measurement error than measurement of concentrations of redox indicators, such as iron and manganese. A cutoff of -90 mV is used herein as a flag to determine where conditions are likely not sufficient for sustained Cr(VI) reduction. This criterion yields the reducing rind boundaries for model layers 1 and 2 in regions where these model layers pass through the fluvial aquifer, as described in the 100% BOD Report, Section 6.4 (Arcadis, 2015).

In contrast, ORP values below -90 mV were not assumed to be sufficient for delineating the reducing rind outside of the fluvial aquifer. Specifically, although ORP values below -90 mV were observed in alluvial wells lining the riverbank, the reducing rind was assumed to stop at the boundary between fluvial and alluvial aquifers. This is based on the observation that the alluvial aquifer does not exhibit the same levels of organic carbon and dissolved iron as the fluvial aquifer. Details regarding correlation between total organic carbon (TOC) and dissolved iron with ORP can be found in the 100% BOD Report (Arcadis, 2015).

3 GROUNDWATER FLOW MODEL DEVELOPMENT

3.1 Model Code Selection and Description

MODFLOW simulates transient, three-dimensional groundwater flow through porous media described by the following partial differential equation for a constant density fluid (Freeze and Cherry, 1979):

$$\frac{\partial}{\partial x} \left(K_{xx} \frac{\partial h}{\partial x} \right) + \frac{\partial}{\partial y} \left(K_{yy} \frac{\partial h}{\partial y} \right) + \frac{\partial}{\partial z} \left(K_{zz} \frac{\partial h}{\partial z} \right) - W = S_s \frac{\partial h}{\partial t} \quad (1)$$

where:

K_{xx} , K_{yy} , and K_{zz} are values of hydraulic conductivity along the x, y, and z coordinate axes, which are assumed to be parallel to the major axes of hydraulic conductivity [L/T]

h is the potentiometric head [L]

W is a volumetric flux and represents sources and/or sinks of water [1/T]

S_s is the specific storage of the porous material [1/L]

t is time [T]

In Equation 1, the hydraulic parameters (i.e., K_{xx} , K_{yy} , K_{zz} , and S_s) may vary in space but not in time, while the source/sink (W) terms may vary both in space and time. The Preconditioned Conjugate Gradient (PCG) solver (Hill, 1990) was used to solve the groundwater flow equation within MODFLOW.

3.2 Model Domain and Grid

The numerical flow model domain is three-dimensional, consisting of 425 rows, 389 columns, and 10 layers. The model domain and grid is presented in Figure 3.2-1. The model consists of 1,653,250 total cells, covering an area of approximately 30,500 acres (47.7 square miles). The grid cell size varies throughout the model domain, with increased resolution in the Site area, with the grid cell size as small as 25 feet by 25 feet. The grid spacing increases up to 200 feet at the model extents. The model grid axes were rotated 45 degrees counter-clockwise to align the major axes of the model with the major direction of anisotropy.

The model was vertically discretized into 10 layers. The bottom of each layer is flat, except for model layers 9 and 10, which vary in elevation, as detailed in Table 3.2-1. Detailed cross sections showing the model layers, planned remedial wells, and monitoring wells are shown in Figures 3.2-2 to 3.2-8.

Table 3.2-1 Model Vertical Structure

Model Layer	Bottom Elevation (ft msl)	Saturated Thickness (ft)
1	425	~30
2	400	25
3	350	50
4	300	50
5	250	50
6	200	50
7	150	50
8	100	50
9	< -200	300+
10	< -500	300

3.3 Boundary Conditions

Boundary conditions must be imposed to define the spatial boundaries of the top, bottom, and all sides of the model grid. Additionally, boundary conditions can be assigned to represent different types of physical

DEVELOPMENT OF GROUNDWATER FLOW AND SOLUTE TRANSPORT MODELS

features, depending on the rules that govern groundwater flow related to the features. The groundwater flow model features 5 types of boundary conditions: no-flow boundary cells, constant-head cells, river cells, constant flux, and pumping wells.

The main source of groundwater beneath Mohave Valley is derived from the Colorado River (Metzger and Loeltz 1973). The river naturally loses water in the northern part of the valley, feeding alluvial aquifers to the east and west. In the southern part of the valley, the regional groundwater of the valley returns to the river as discharge as the aquifer thins southward. At Needles, a portion of the Colorado River flow is diverted to Topock Marsh. The water supports wetlands over an 8-mile stretch to the east of the river, and the excess water returns to the river either by direct flow or by infiltration into groundwater. The model domain cuts through the northern portion of the marsh, and a constant head boundary is assigned for the northern boundary. River cells were used to simulate the Colorado River and the Topock Bay and Topock Marsh. The river stages in the Topock Bay and Marsh were held constant and corresponds to the average head maintained by the Havasu National Wildlife Refuge, as reported in Guay (2001). The stage of the Colorado River was determined by average stage values measured at I-3 and interpolated based on gradients determined between Davis Dam and Parker Dam. River bed elevations were based on the river seismic survey data and extending the observed slope into areas where no data were collected (CH2M Hill, 2006b).

On the west side of the river, groundwater enters the model at the northern boundary to simulate regional down-valley flow and exits at the river (natural discharge). The regional down-valley flow is simulated as a constant head boundary condition along the northwestern model boundary. This provides a constant southward flux of water into the model domain. A constant head condition was used because the flow into the northern model area is regionally-derived, providing a relatively large amount of water that is not assumed to be affected by pumping conditions within the model domain. The head value used in the model corresponds to the estimated river level at the model boundary. A constant head boundary condition is also assigned to the narrow section of aquifer that exists directly beneath the river channel on the southern model boundary (CH2M Hill, 2006b). The remainder of the southern boundary is assigned as a no-flow boundary because it is all considered competent bedrock, which is assumed to allow very limited groundwater flow (Metzger and Loeltz 1973).

The majority of the eastern and western boundaries of the model are assigned as no-flow boundaries, since they are essentially parallel to the regional flow direction. One exception is a short section of constant flux boundaries used to simulate underflows associated with washes that enter the model domain from the west in the alluvium. This type of boundary condition is assigned in cases where either the flux is considered to be well-quantified or is assumed to be relatively small (i.e. non-regional). The latter condition determined the constant flux condition in the case of this model (CH2M Hill, 2006b). Another exception is the simulation of constant flux boundaries assigned in the southwestern extent of the model to represent the groundwater flux received from precipitation in the Chemehuevi Mountains located to the south of the Site. Pumping wells simulating the regional extraction wells for Golden Shores, Topock 2, Topock 3, and Park Moabi were also incorporated in the model. Boundary conditions are shown for model layer 1 in Figure 3.3-1.

3.4 Hydraulic Parameters

3.4.1 Hydraulic Conductivity

The interpolated bedrock surface elevation and the thicknesses of the hydrostratigraphic units were utilized to determine where the individual hydrostratigraphic units intercepted the revised model layer structure. The hydrostratigraphic unit extents present in each model layer were used to define the hydraulic conductivity zonation. The hydrostratigraphic units for each model layer are shown in Figures 3.4-1 to Figure 3.4-2. Initial hydraulic conductivity values for the individual hydrostratigraphic units were assigned based on available aquifer test data. These initial values were further refined during the calibration process through manual adjustment and automatic parameter estimation using PEST. Hydraulic conductivity was allowed to vary within the range of recorded aquifer test values and previously modelled values using professional judgment. As there was limited regional hydraulic conductivity data available for the full model domain and the majority of the calibration targets are located in the immediate vicinity of the Site, the regional hydraulic conductivity values were dependent on the available Site data. The initial calibration of the model to single hydraulic conductivity values for each hydrostratigraphic unit was then allowed to vary within each hydrostratigraphic unit by generating a stochastic distribution of hydraulic conductivity. A two-dimensional spatially correlated log normal conductivity field was generated for the model using a Gaussian power spectrum (Robin et al, 1993). The distribution was constrained within the range of potential hydraulic conductivity values and the distribution was varied by layer to represent the vertical heterogeneity between hydrostratigraphic units that span multiple model layers. While the hydraulic conductivity pattern and values varied within each hydrostratigraphic unit, the average value for each hydrostratigraphic unit was still consistent with calibrated values. The use of these random generated fields allows for potential uncertainties associated with heterogeneities encountered in the aquifer while maintaining a well calibrated model. The hydraulic conductivity distributions per model layer are shown in Figures 3.4-3 to 3.4-4. Vertical hydraulic conductivity was not a sensitive parameter during the calibration and sensitivity analyses, so a horizontal to vertical hydraulic conductivity ratio of 10:1 was utilized throughout the model domain.

3.4.2 Evapotranspiration

Direct evapotranspiration of groundwater is also modeled with a specific outward flux assigned to selected model nodes that varies with depth of the water table from land surface. A maximum evapotranspiration flux is assigned to each node, along with an "extinction depth," which is the depth beneath the ground surface at which evapotranspiration flux equals zero. This is usually assumed to be the maximum effective root depth for plants in the area. The flux of water actually removed from each nodal area depends on the depth of the water table at that location. The maximum assigned evapotranspiration rate is applied when the water table elevation equals the land surface. Calculated flux decreases linearly from the maximum flux at ground surface to zero at the extinction depth. The water table must be above the extinction depth for any water to be removed by evapotranspiration in the simulations. A nominal maximum evapotranspiration rate has been applied to all model nodes, but only nodes close to the Colorado River have a water table depth shallow enough for evapotranspiration to be active. A greater maximum evapotranspiration rate has been assigned in areas of more dense vegetation,

notably the mouth of Bat Cave Wash and the southern part of the floodplain (CH2M Hill, 2006b). The evapotranspiration distribution is shown in Figure 3.4-5.

3.4.3 Recharge

Rainfall associated with the Chemehuevi Mountains area was accounted for using constant flux boundaries in the southwest corner of the groundwater flow model. In the mountain areas of the model, all layers are assigned bedrock properties. Recharge in these areas is assumed to infiltrate through fractures and weathered bedrock surfaces and emerge near the mountain front. The model allows flow through the bedrock unit, eventually intersecting the more permeable alluvial HSUs to the north of the recharge area. This recharge mechanism results in a mildly upward gradient into the alluvium, as observed on the site at well cluster MW-24. No rainfall recharge is assigned to other areas of the model because the very small amount of rainfall in the lower elevations (less than 5 inches per year) is assumed to evaporate before infiltrating to groundwater (CH2M Hill, 2006b). The published estimate of rainfall in the mountain areas is around 10 inches per year (Metzger and Loeltz 1973), and 1 to 2 percent of this rainfall is assumed to infiltrate either directly into bedrock or into alluvium as mountain front recharge.

3.5 Groundwater Flow Model Calibration

Calibration of a groundwater flow model refers to the process of adjusting model parameters to obtain a reasonable match between observed and simulated water levels. Model calibration is an iterative procedure that involves adjustment of hydraulic properties and/or boundary conditions to achieve the best match between observed and simulated water levels. During model calibration, model parameters are varied over a narrow range set by Site-specific data using the CSM as a guide. During calibration of a groundwater flow model, use of point data (targets) eliminates the potential for interpretive bias that may result from attempting to match a contoured potentiometric surface (Konikow, 1978; Anderson and Woessner, 1992). The groundwater flow model was calibrated under steady state and transient conditions, presented in the following sections.

3.5.1 Steady State Calibration

The steady-state flow calibration process for the numerical model consisted of two different time periods: Pre IM-3 Conditions in 2004 and Active IM-3 Conditions in 2015. The Pre IM-3 Pumping Conditions consisted of pumping conditions described in Section 3.3. The Pre IM-3 Conditions consisted of 26 groundwater elevation targets measured at monitoring wells on-Site in 2004 (Table 3.5-1). The Active IM-3 Pumping conditions represent the average 2015 rates and consisted of the addition of 4 pumping wells: IW-2 (screened in model layers 3 through 6) injecting at a total rate of 66.3 gpm), IW-3 (screened in model layers 3 through 6) injecting at a total rate of 61.6 gpm), PE-1 (screened in model layer 3 extracting at a total rate of 26 gpm), and TW-3D (screened in model layers 3 through 4 extracting at a total rate of 102.7 gpm). The Active IM-3 Conditions consisted of 71 groundwater elevation targets measured at monitoring wells on-Site (Table 3.5-2). The Active IM-3 targets were measured over the course of 2015 and averaged.

DEVELOPMENT OF GROUNDWATER FLOW AND SOLUTE TRANSPORT MODELS

Table 3.5-1 Pre IM-3 Water Level Targets and Residuals

Name	X	Y	Layer	Observed Water Level (ft msl)	Computed Water Level (ft msl)	Residual (ft)
MW-09	7614780.27	2100673.29	1	456.46	456.05	0.41
MW-10	7614886.60	2100984.20	1	455.35	455.99	-0.64
MW-11	7614865.33	2101557.09	1	455.75	455.91	-0.16
MW-12	7615923.61	2101429.49	1	455.71	455.74	-0.03
MW-13	7614848.07	2103135.17	1	456.15	455.70	0.45
MW-14	7614081.09	2102738.09	1	455.86	455.90	-0.04
MW-15	7613164.94	2100844.08	1	456.08	456.31	-0.23
MW-20-070	7615893.48	2102493.39	1	455.35	455.48	-0.13
MW-21	7616099.26	2101486.75	1	455.48	455.66	-0.18
MW-22	7616359.75	2101566.69	1	454.58	455.33	-0.75
MW-23	7616448.53	2101286.15	1	455.21	456.15	-0.94
MW-24A	7615114.47	2101451.00	1	455.50	455.89	-0.39
MW-27-020	7616557.66	2102294.73	1	455.75	455.22	0.53
MW-30-030	7616141.26	2102499.58	1	455.35	455.38	-0.03
MW-16	7610980.32	2100697.20	1	456.47	456.73	-0.26
MW-17	7610243.29	2103135.56	1	455.73	456.48	-0.75
MW-18	7612598.61	2102894.59	1	455.70	456.13	-0.43
MW-20-100	7615881.03	2102506.33	2	455.22	455.48	-0.26
MW-30-050	7616150.98	2102503.83	2	455.12	455.38	-0.26
MW-34-055	7616444.49	2102542.45	2	455.23	455.28	-0.05
PGE-06	7615050.86	2101525.07	2	455.76	455.89	-0.13
MW-20-130	7615881.52	2102493.68	3	455.53	455.48	0.05
MW-24B	7615069.38	2101436.41	3	455.98	455.90	0.08
MW-34-080	7616444.98	2102535.25	3	455.47	455.28	0.19
IW-03	7613237.80	2103007.18	4	455.17	456.02	-0.85
PGE-07	7615034.78	2101350.19	4	456.50	457.13	-0.63
Residual Statistics						
Residual Mean (ft)						-0.209
Residual Std. Deviation (ft)						0.383
Sum of Squares (ft ²)						4.940
Number of Observations						26
Range in Observations (ft)						1.920
Scaled Residual Std. Deviation						0.199

DEVELOPMENT OF GROUNDWATER FLOW AND SOLUTE TRANSPORT MODELS

Table 3.5-2 Active IM-3 Water Level Targets and Residuals

Name	X	Y	Layer	Observed Water Level (ft msl)	Computed Water Level (ft msl)	Residual (ft)
MW-10	7614886.60	2100984.20	1	455.45	455.99	-0.54
MW-11	7614865.33	2101557.09	1	455.90	455.89	0.01
MW-12	7615923.61	2101429.49	1	455.51	455.52	0.00
MW-20-070	7615893.48	2102493.39	1	454.02	454.51	-0.49
MW-21	7616099.26	2101486.75	1	455.24	455.41	-0.17
MW-22	7616359.75	2101566.69	1	454.96	455.13	-0.17
MW-23-060	7616448.25	2101286.36	1	455.24	456.03	-0.79
MW-23-080	7616448.50	2101286.33	1	455.32	456.04	-0.71
MW-25	7615303.59	2102351.22	1	455.45	455.34	0.11
MW-26	7615787.70	2101911.86	1	455.15	455.24	-0.09
MW-27-020	7616557.66	2102294.73	1	455.21	455.01	0.20
MW-28-025	7616280.73	2103003.90	1	455.16	455.06	0.10
MW-30-030	7616141.26	2102499.58	1	454.80	454.62	0.18
MW-32-035	7616306.62	2102034.68	1	454.93	454.96	-0.03
MW-33-040	7615916.42	2103280.79	1	455.02	455.15	-0.13
MW-35-060	7615317.50	2104058.80	1	455.56	455.53	0.03
MW-36-020	7616267.10	2102542.57	1	454.92	454.68	0.23
MW-36-040	7616267.58	2102537.20	1	454.88	454.68	0.19
MW-38S	7614918.75	2101279.65	1	454.95	455.93	-0.98
MW-39-040	7616091.44	2102506.22	1	454.71	454.59	0.13
MW-42-030	7616282.09	2102309.31	1	454.84	454.77	0.07
MW-43-025	7616702.79	2101817.51	1	455.13	455.08	0.05
MW-47-055	7615629.48	2103450.05	1	455.43	455.36	0.07
OW-01S	7613419.20	2103040.48	1	456.55	456.87	-0.32
OW-02S	7613373.76	2103153.89	1	456.57	456.86	-0.28
OW-05S	7613186.80	2103017.60	1	456.61	456.91	-0.31
MW-20-100	7615881.03	2102506.33	2	453.53	454.35	-0.81
MW-27-060	7616534.75	2102288.27	2	455.09	454.97	0.13
MW-30-050	7616150.98	2102503.83	2	454.86	454.59	0.27
MW-33-090	7615914.59	2103287.43	2	455.29	455.17	0.12
MW-34-055	7616444.49	2102542.45	2	455.09	454.83	0.26
MW-36-050	7616267.47	2102532.17	2	454.81	454.63	0.19
MW-36-070	7616267.18	2102542.67	2	454.84	454.62	0.21
MW-37S	7614827.87	2102869.45	2	455.17	455.71	-0.54
MW-39-050	7616095.96	2102498.75	2	454.57	454.55	0.02

DEVELOPMENT OF GROUNDWATER FLOW AND SOLUTE TRANSPORT MODELS

MW-39-060	7616099.45	2102495.05	2	454.40	454.56	-0.16
MW-39-070	7616091.38	2102506.30	2	454.09	454.54	-0.45
MW-44-070	7616255.62	2102728.31	2	454.97	454.76	0.21
MW-50-095	7615599.84	2103069.27	2	455.22	455.15	0.07
MW-55-045	7618326.30	2102605.89	2	456.09	455.26	0.83
MW-20-130	7615881.52	2102493.68	3	453.37	454.18	-0.80
MW-27-085	7616540.34	2102290.53	3	455.07	454.95	0.12
MW-28-090	7616289.73	2103005.68	3	455.15	455.03	0.12
MW-31-135	7615819.13	2102835.29	3	454.21	454.48	-0.26
MW-34-080	7616444.98	2102535.25	3	455.16	454.71	0.45
MW-34-100	7616452.41	2102530.60	3	454.86	454.74	0.12
MW-35-135	7615329.76	2104045.82	3	455.76	455.54	0.22
MW-36-090	7616267.63	2102537.34	3	453.97	454.45	-0.48
MW-36-100	7616267.51	2102532.37	3	454.23	454.46	-0.23
MW-39-080	7616095.86	2102498.83	3	454.08	454.48	-0.40
MW-39-100	7616099.30	2102494.96	3	454.56	454.49	0.07
MW-42-065	7616274.98	2102296.96	3	454.76	454.70	0.06
MW-43-090	7616693.22	2101824.65	3	455.48	455.08	0.40
MW-44-115	7616262.10	2102723.85	3	454.55	454.72	-0.17
MW-44-125	7616255.55	2102728.48	3	455.03	454.72	0.31
MW-45-095a	7616358.12	2102559.75	3	453.85	453.84	0.01
MW-45-095B	7616358.12	2102559.75	3	453.86	453.84	0.01
MW-47-115	7615629.75	2103450.10	3	455.46	455.36	0.10
MW-49-135	7615889.63	2103667.52	3	455.40	455.34	0.06
MW-51	7615807.51	2101900.11	3	455.04	455.23	-0.19
MW-54-085	7617082.61	2102958.94	3	455.52	455.21	0.31
MW-55-120	7618326.13	2102606.18	3	456.07	455.26	0.81
PT2D	7616017.74	2102646.24	3	453.90	454.26	-0.36
PT5D	7616112.09	2102629.47	3	454.33	454.48	-0.14
PT6D	7616074.62	2102672.77	3	454.30	454.43	-0.13
MW-33-150	7615906.05	2103302.57	4	455.21	455.22	-0.01
MW-46-175	7616196.86	2102940.02	4	455.11	454.95	0.15
MW-54-140	7617082.16	2102959.12	4	455.90	455.21	0.69
OW-05M	7613185.86	2103008.06	4	457.46	457.24	0.22
MW-54-195	7617089.25	2102951.90	5	455.92	455.22	0.70
OW-05D	7613185.55	2102998.32	6	457.16	457.20	-0.04
Residual Statistics						
Residual Mean (ft)						-0.023

DEVELOPMENT OF GROUNDWATER FLOW AND SOLUTE TRANSPORT MODELS

Residual Std. Deviation (ft)	0.358
Sum of Squares (ft ²)	9.118
Number of Observations	71.000
Range in Observations (ft)	4.086
Scaled Residual Std. Deviation	0.088

3.5.1.1 Pre IM-3 Conditions

The quality of the model calibration can be determined by a statistical analysis of the residuals, as shown in Table 3.5-1. Residuals are defined as the difference between the model-simulated heads and the observed values. Positive residual values indicate that the model-simulated values are lower than the measured values, and negative residual values indicate that the model-simulated values are higher than the measured values. Residual statistics (Table 3.5-1) for the calibrated groundwater flow model indicate an acceptable agreement between simulated and measured groundwater elevations. The residual mean, residual standard deviation, and sum of squared residuals were calculated to be -0.209 feet, 0.383 feet, and 4.940 square feet (ft²), respectively. The residual standard deviation is less than 20% of the range in observed water levels. These statistics indicate a good agreement between the observed and simulated water levels. A plot of observed versus simulated groundwater elevations for the 26 calibration targets is presented on Figure 3.5-1. The Pre IM-3 Conditions were considered a validation of the model calibration rather than the primary target set since Site 2004 data was fairly limited. The simulated layer-wise and full model water budget is shown in table 3.5-3

Table 3.5-3 Pre IM-3 Conditions Water Balance

Description	Model Layer 1		Model Layer 2		Model Layer 3		Model Layer 4		Model Layer 5	
	Inflow (ft ³ /day)	Outflow (ft ³ /day)	Inflow (ft ³ /day)	Outflow (ft ³ /day)	Inflow (ft ³ /day)	Outflow (ft ³ /day)	Inflow (ft ³ /day)	Outflow (ft ³ /day)	Inflow (ft ³ /day)	Outflow (ft ³ /day)
Constant Flux	1,326	0	14,924	0	5,543	0	0	0	0	0
ET	0	97,335	0	0	0	0	0	0	0	0
Constant Head	2,969	2,075	2,074	1,417	3,766	2,573	4,330	2,361	4,254	2,159
River	376,923	310,063	0	0	0	0	0	0	0	0
Well	0	11,849	0	9,461	0	418	0	256	0	2,887
Storage	0	0	0	0	0	0	0	0	0	0
TOTAL	683,095	682,785	576,407	576,407	484,205	484,205	400,268	400,268	328,602	328,602
ERROR	4.55E-02		3.69E-06		-6.71E-07		1.49E-06		2.86E-06	
Description	Model Layer 6		Model Layer 7		Model Layer 8		Model Layer 9		Model Layer 10	
	Inflow (ft ³ /day)	Outflow (ft ³ /day)	Inflow (ft ³ /day)	Outflow (ft ³ /day)	Inflow (ft ³ /day)	Outflow (ft ³ /day)	Inflow (ft ³ /day)	Outflow (ft ³ /day)	Inflow (ft ³ /day)	Outflow (ft ³ /day)

DEVELOPMENT OF GROUNDWATER FLOW AND SOLUTE TRANSPORT MODELS

Constant Flux	0	0	0	0	0	0	0	0	0	0
ET	0	0	0	0	0	0	0	0	0	0
Constant Head	2,729	762	3,359	853	3,260	990	97,779	44,439	1	36
River	0	0	0	0	0	0	0	0	0	0
Well	0	3,764	0	1,046	0	871	0	49	0	0
Storage	0	0	0	0	0	0	0	0	0	0
TOTAL	275,314	275,314	241,653	241,653	204,124	204,124	160,701	160,701	96	96
ERROR	4.74E-07		1.83E-06		3.06E-06		3.21E-05		2.07E-01	
Description	FULL MODEL									
	Inflow (ft³/day)	Outflow (ft³/day)								
Constant Flux	21,794	0								
ET	0	97,368								
Constant Head	124,522	57,663								
River	342,967	303,340								
Well	0	30,601								
Storage	0	0								
TOTAL	489,283	488,972								
ERROR	6.36E-02									

3.5.1.2 Active IM-3 Conditions

To simulate active IM-3 conditions, the observed water levels Residual statistics (Table 3.5-2) for the calibrated groundwater flow model indicate an acceptable agreement between simulated and measured groundwater elevations. The residual mean, residual standard deviation, and sum of squared residuals were calculated to be -0.023 feet, 0.358 feet, and 9.121ft², respectively. The residual standard deviation is less than 9% of the range in observed water levels. These statistics indicate a good agreement between the observed and simulated water levels. A plot of observed versus simulated groundwater elevations for the 72 calibration targets is presented on Figure 3.5-2. The simulated layerwise and full model water budget is shown in Table 3.5-4. The model calibration process focused more on the active IM-3 conditions (2015) rather than pre-IM-3 conditions (2004) because substantially more data was available in 2015 and water levels were more reflective of annual average levels.

Table 3.5-4 Active IM-3 Conditions Water Balance

Description	Model Layer 1		Model Layer 2		Model Layer 3		Model Layer 4		Model Layer 5	
	Inflow (ft ³ /day)	Outflow (ft ³ /day)	Inflow (ft ³ /day)	Outflow (ft ³ /day)	Inflow (ft ³ /day)	Outflow (ft ³ /day)	Inflow (ft ³ /day)	Outflow (ft ³ /day)	Inflow (ft ³ /day)	Outflow (ft ³ /day)

DEVELOPMENT OF GROUNDWATER FLOW AND SOLUTE TRANSPORT MODELS

Constant Flux	1,326	0	14,924	0	5,543	0	0	0	0	0
ET	0	97,366	0	0	0	0	0	0	0	0
Constant Head	2,962	2,075	2,069	1,417	3,758	2,573	4,322	2,361	4,246	2,160
River	348,722	308,620	0	0	0	0	0	0	0	0
Well	0	11,862	0	9,448	3,955	19,801	8,221	5,658	7,816	2,895
Storage	0	0	0	0	0	0	0	0	0	0
TOTAL	698,101	697,790	597,132	597,132	514,602	514,602	421,841	421,841	345,259	345,259
ERROR	4.45E-02		2.85E-06		-1.19E-07		9.31E-07		2.52E-06	
Description	Model Layer 6		Model Layer 7		Model Layer 8		Model Layer 9		Model Layer 10	
	Inflow (ft³/day)	Outflow (ft³/day)	Inflow (ft³/day)	Outflow (ft³/day)	Inflow (ft³/day)	Outflow (ft³/day)	Inflow (ft³/day)	Outflow (ft³/day)	Inflow (ft³/day)	Outflow (ft³/day)
Constant Flux	0	0	0	0	0	0	0	0	0	0
ET	0	0	0	0	0	0	0	0	0	0
Constant Head	2,722	762	3,351	853	3,252	990	97,573	44,495	1	36
River	0	0	0	0	0	0	0	0	0	0
Well	4,640	3,775	0	1,049	0	873	0	25	0	0
Storage	0	0	0	0	0	0	0	0	0	0
TOTAL	286,025	286,025	245,695	245,695	204,911	204,911	160,278	160,278	97	96
ERROR	1.30E-06		1.95E-06		3.52E-06		2.75E-05		1.98E-01	
Description	FULL MODEL									
	Inflow (ft³/day)	Outflow (ft³/day)								
Constant Flux	21,794	0								
ET	0	97,366								
Constant Head	124,257	57,723								
River	348,722	308,620								
Well	24,632	55,385								
Storage	0	0								
TOTAL	519,405	519,094								
ERROR	5.99E-02									

3.5.2 Transient Calibration

The transient calibration was conducted with 827 water level targets from November 2014 to October 2015. Average variations in the Colorado River stage and pumping were computed on a monthly basis. As the transient calibration model is a time dependent simulation, storativity (storage) needed to be incorporated into the model. Storage values were varied per hydrostratigraphic unit. The calibrated storativity values for the individual hydrostratigraphic units are shown in Table 3.5-5. In general, storativity was not a sensitive parameter in matching the transient calibration period, so the values in Table 3.5-5

should be considered approximations. As the solute transport modelling is conducted as a long term steady state run, the storage values are not used in the solute transport model.

Table 3.5-5 Hydrostratigraphic Unit Storativity Values

Hydrostratigraphic Unit	Description	Average Storativity Value
Qr3	Upper Fluvial Sand and Silt	6.5E-02
Qr2	Middle Fluvial Deposits	1.9E-02
Qr1	Lower Fluvial Deposits	1.4E-02
Qr0	Colorado River Channel Fill	1.5E-02
Qoa	Older Quarternary Alluvium	5.1E-2
Tb	Bouse Formation	6.0E-2
Toa2	Upper Tertiary Alluvium	1.9E-02
Toa1	Lower Tertiary Alluvium	8.1E-05
Toa0	Basal Alluvium	2.8E-05
Tmc	Miocene Conglomerate	2.2E-04

Residual statistics (Appendix A) for the calibrated groundwater flow model indicate an acceptable agreement between simulated and measured groundwater elevations. The residual mean, residual standard deviation, and sum of squared residuals were calculated to be 0.16 feet, 0.42 feet, and 169.0ft², respectively. The residual standard deviation is 6% of the range in observed water levels. These statistics indicate a good agreement between the observed and simulated water levels. A plot of observed versus simulated groundwater elevations for the 827 calibration targets is presented on Figure 3.5-3. Example hydrographs for the floodplain and upland areas are shown in Figures 3.5-4 and 3.5-5, respectively. Each hydrograph shows good fit between observed and simulated conditions as the river stage and IM-3 pumping rates varied over time.

3.6 Simulated Groundwater Flow

The simulated water levels under the Active IM-3 Conditions were mapped both regionally and for the Site and are presented in Figures 3.6-1 and 3.6-2, respectively. Regionally, groundwater flow is from

north to south. Due to the contrast in permeabilities between the alluvium and the bedrock, the gradient steepens in the bedrock located to the south of the Site. At the Site, mounding and drawdown is evident due to local IM-3 pumping at the injection and extraction wells (IW-2, IW-3, PE-1, and TW-3D). In the vicinity of the Site, groundwater flow is predominantly to the east towards the Colorado River. In the bedrock, groundwater travels from south to north out of the bedrock and into the alluvium.

3.7 Sensitivity Analyses

Sensitivity analyses were conducted on the following parameters: hydraulic conductivity, riverbed conductance, leakance, and evapotranspiration. The 2015 steady state calibration model was utilized to conduct this sensitivity analysis. The sensitivity of the model to global changes in parameters is presented graphically in Figure 3.7-1. The layerwise sensitivity analysis of leakance is presented graphically in Figure 3.7-2. Additional details on the sensitivity analysis are discussed in the sections below.

3.7.1 Hydraulic Conductivity

Hydraulic conductivity values were varied globally by applying a range of multipliers between 0.5 and 1.75 and the resultant statistics are presented in Table 3.7-1. The majority of the targets are located in the immediate vicinity of the Site, but the parameters were varied across the full model domain to gauge the overall impact. Based on the calibration statistics, the hydraulic conductivity value is a relatively sensitive parameter. Within a 5% increase and decrease in hydraulic conductivity the calibration had minimal changes. As the multiplier was increased and decreased further, the deviation from the base calibration statistics increased significantly. Due to the heterogeneous nature of the stochastic distribution of simulated hydraulic conductivity values, further discrete sensitivity analyses were not conducted on hydraulic conductivity.

Table 3.7-1 Hydraulic Conductivity Sensitivity Analysis

Residual Statistics	Hydraulic Conductivity										
	0.50	0.75	0.85	0.90	0.95	1.00	1.05	1.15	1.25	1.50	1.75
Multiplier	0.50	0.75	0.85	0.90	0.95	1.00	1.05	1.15	1.25	1.50	1.75
Residual Mean (ft)	0.227	0.067	0.026	0.008	-0.008	-0.023	-0.037	-0.061	-0.083	-0.128	-0.163
Residual Std. Deviation (ft)	0.665	0.405	0.372	0.364	0.359	0.358	0.358	0.364	0.374	0.402	0.430
Sum of Squares (ft ²)	35.07	11.98	9.881	9.397	9.164	9.118	9.212	9.690	10.41	12.65	15.00
Scaled Residual Std. Deviation	0.163	0.099	0.091	0.089	0.088	0.088	0.088	0.089	0.091	0.098	0.105

3.7.2 Riverbed Conductance

Riverbed conductance values were varied globally in all river cells by applying a range of multipliers between 0.1 and 10 and the resultant statistics are presented in Table 3.7-2. Riverbed conductance values had a relatively low degree of sensitivity with only a slight increase in residual statistics when riverbed conductance values were reduced beyond a 0.75 multiplier. Increasing the riverbed conductance did not result in a significant improvement of calibration statistics. The asymptotic nature of this sensitivity curve supports the baseline riverbed conductance value utilized for the model calibration.

Table 3.7-2 Riverbed Conductance Sensitivity Analysis

Residual Statistics	Riverbed Conductance							
Multiplier	0.10	0.50	0.75	1.00	1.25	1.50	1.75	10.00
Residual Mean (ft)	-0.014	-0.016	-0.020	-0.023	-0.025	-0.026	-0.028	-0.037
Residual Std. Deviation (ft)	0.377	0.360	0.358	0.358	0.357	0.357	0.356	0.355
Sum of Squares (ft ²)	10.092	9.232	9.152	9.118	9.093	9.080	9.070	9.041
Scaled Residual Std. Deviation	0.092	0.088	0.088	0.088	0.087	0.087	0.087	0.087

3.7.3 Evapotranspiration

Evapotranspiration rates were varied uniformly across the full model domain by applying multipliers from 0.1 to 10 and resultant statistics are presented in Table 3.7-3. Although evapotranspiration zones were defined throughout the model domain, due to the relatively large depth to water and limited vegetation in the uplands, this parameter was really only active in the Colorado River floodplain and Topock Marsh areas as this is where the groundwater is relatively shallow and vegetation exists. This sensitivity analysis indicates that evapotranspiration is a relatively insensitive parameter. Decreasing the evapotranspiration rate had little to no impact of the residual calibration statistics. Only by increasing the evapotranspiration rate by an order of magnitude resulted in a larger increase in calibration statistics.

Table 3.7-3 Evapotranspiration Sensitivity Analysis

Residual Statistics	Evapotranspiration							
Multiplier	0.10	0.50	0.75	1.00	1.25	1.50	1.75	10.00
Residual Mean (ft)	-0.031	-0.027	-0.025	-0.023	-0.021	-0.019	-0.017	0.047
Residual Std. Deviation (ft)	0.362	0.360	0.359	0.358	0.356	0.355	0.354	0.333
Sum of Squares (ft ²)	9.389	9.263	9.189	9.118	9.050	8.985	8.923	8.031
Scaled Residual Std. Deviation	0.089	0.088	0.088	0.088	0.087	0.087	0.087	0.081

3.7.4 Leakance

Leakance rates were first varied uniformly across the full model domain in all model layers by applying multipliers from 0.1 to 10 and resultant statistics are presented in Table 3.7-4. In general leakance was fairly insensitive until the leakance values were increased or decreased by an order of magnitude. The base leakance value had the lowest residual sum of squares and scaled residual standard deviation supporting the calibration values suggested.

Table 3.7-4 Leakance Sensitivity Analysis

Residual Statistics	Leakance							
Multiplier	0.10	0.50	0.75	1.00	1.25	1.50	1.75	10.00
Residual Mean (ft)	-0.006	-0.021	-0.022	-0.023	-0.024	-0.025	-0.026	-0.040
Residual Std. Deviation (ft)	0.422	0.360	0.358	0.358	0.358	0.358	0.359	0.365
Sum of Squares (ft ²)	12.642	9.243	9.131	9.118	9.132	9.155	9.181	9.600
Scaled Residual Std. Deviation	0.103	0.088	0.088	0.088	0.088	0.088	0.088	0.089

To further evaluate the leakance rates in the model, the individual leakance values between model layers 1 through 3 were varied independently to gauge the relative sensitivity by layer. Layers 1 through 3 were selected as these were the layers containing the majority of the calibration targets. Leakance in each layer was varied between 0.1 and 10 times the baseline leakance value and the resultant calibration statistics are shown in Table 3.7-5 and are depicted graphically in Figure 3.7-2. The overall conclusions between the global leakance variations and layerwise leakance variations are similar indicating that leakance is a relatively insensitive parameter.

Table 3.7-5 Layerwise Leakance Sensitivity Analysis

Residual Statistics	Leakance Model layer 1							
Multiplier	0.10	0.50	0.75	1.00	1.25	1.50	1.75	10.00
Residual Mean (ft)	-0.020	-0.017	-0.020	-0.023	-0.025	-0.027	-0.026	-0.039
Residual Std. Deviation (ft)	0.362	0.357	0.357	0.358	0.358	0.358	0.359	0.363
Sum of Squares (ft ²)	9.340	9.081	9.094	9.118	9.144	9.169	9.181	9.472
Scaled Residual Std. Deviation	0.089	0.087	0.087	0.088	0.088	0.088	0.088	0.089
Residual Statistics	Leakance Model layer 2							
Multiplier	0.10	0.50	0.75	1.00	1.25	1.50	1.75	10.00
Residual Mean (ft)	-0.052	-0.025	-0.024	-0.023	-0.023	-0.023	-0.023	-0.026
Residual Std. Deviation (ft)	0.399	0.357	0.357	0.358	0.358	0.359	0.359	0.365
Sum of Squares (ft ²)	11.498	9.110	9.091	9.118	9.150	9.181	9.208	9.501
Scaled Residual Std. Deviation	0.098	0.087	0.087	0.088	0.088	0.088	0.088	0.089
Residual Statistics	Leakance Model layer 3							
Multiplier	0.10	0.50	0.75	1.00	1.25	1.50	1.75	10.00

Residual Mean (ft)	-0.045	-0.025	-0.023	-0.023	-0.023	-0.023	-0.023	-0.026
Residual Std. Deviation (ft)	0.362	0.359	0.358	0.358	0.357	0.357	0.357	0.357
Sum of Squares (ft ²)	9.465	9.175	9.137	9.118	9.107	9.099	9.095	9.092
Scaled Residual Std. Deviation	0.089	0.088	0.088	0.088	0.087	0.087	0.087	0.087

4 SOLUTE TRANSPORT MODEL DEVELOPMENT

Solute transport modeling was performed to evaluate the migration and fate of Cr(VI) detected in the groundwater, as well as the fate and transport of potential IRZ byproducts (i.e., manganese and arsenic). The solute transport model used the results from the calibrated groundwater flow model to simulate solute transport under average flow conditions. The solute transport model was used to evaluate the fate and transport of Cr(VI), as well as select byproducts (manganese and arsenic) to evaluate various potential remedial systems.

4.1 Code Selection

The solute transport modeling was performed using the modular three-dimensional transport model referred to as MT3D. MT3D was originally developed by Zheng (1990) at S.S. Papadopoulos & Associates, Inc. for the Robert S. Kerr Environmental Research Laboratory of the U.S. Environmental Protection Agency (USEPA). The MT3D code uses the flows computed by MODFLOW in its transport calculations. MT3D also uses the same finite-difference grid structure and boundary conditions as MODFLOW, simplifying the effort to construct the solute transport model. MT3D is regularly updated (Zheng and Wang 1999), and the most recent version is referred to in the literature as MT3DMS, where MS denotes the Multi-Species structure for accommodating add-on reaction packages. MT3DMS has a comprehensive set of options and capabilities for simulating advection, dispersion/diffusion, and chemical reactions of contaminants in groundwater flow systems under a range of hydrogeologic conditions. Recent updates to MT3DMS have included the dual-domain formulation and the ability to incorporate Site-specific processes.

The major inputs to MT3DMS for the modeling assessment are as follows:

- Mobile and Immobile Porosity: affecting the groundwater flow velocity and solute storage
- Mass Transfer Coefficient: affecting the exchange of mass between mobile and immobile portions of the aquifer
- Partition Coefficient: affecting the adsorption of Cr(VI) and byproducts to soil particles
- Carbon Degradation Rate: affecting the rate of Cr(VI) reduction/precipitation
- Initial Groundwater Concentrations: affecting the overall distribution and concentration of Cr(VI), manganese, and arsenic

- Byproduct Generation Coefficient: affecting the generation of manganese and arsenic from the introduction of carbon to aquifer

4.2 Solute Transport Parameters

4.2.1 Porosity

The first phase of calibration was to accurately represent the groundwater velocity in the impacted portion of the aquifer. The groundwater velocity is computed within MT3DMS by dividing the groundwater flux term from MODFLOW by the mobile porosity. The mobile porosity is that fraction of the aquifer through which the majority of groundwater is moving. While often conceptualized as solely a pore-scale concept, it also represents aquifer-scale behavior driven by hydraulic conductivity contrasts in different portions of the aquifer matrix. The immobile porosity is the remaining portion of the void space, where groundwater flows much slower or not at all, and the void space is primarily a storage reservoir for dissolved mass. Solute mass is exchanged between mobile and immobile portions of the aquifer by diffusion. This conceptualization of solute transport is the dual-domain formulation, and is often referred to as advection-diffusion. There is extensive literature on the dual-domain model (Gillham et al. 1984; Molz et al. 2006; Flach et al. 2004; Harvey and Gorelick 2000; Feehley et al. 2000; Julian et al. 2001; Zheng and Bennet 2002) and it is generally considered the most accurate approach for simulating solute transport.

The total (combination of mobile and immobile) porosity of the aquifer is controlled by grain sizes, sorting, and post-depositional consolidation processes. Attachment A of CH2M Hill 2010 - Methods of Estimating Pore Volume Flushing Efficiency Used in Calculating Mass Removal Rates for CMS/FS Alternative indicated a range in immobile porosities of 22% to 28%, and a range in total porosities of 29% to 40%. The total porosity range is supported by porosity measurements made on 20 Site samples as part of the original draft RFI (E&E, 2004), which ranged between 26.8% and 42.7%, with an average of 35.5%. A mobile porosity of 12% was determined through Site ISPT tracer studies (Arcadis, 2008) (see Section 3.4.4), including the breakthrough of IM-3 injection water. Based on this 12% mobile porosity, an immobile porosity of 23% and a total porosity of 35% were selected as average values for the solute transport modeling exercise to be consistent with the calculated ranges in observed immobile and total porosities. The total porosity of 35% is also consistent with porosity values recorded for similar alluvial and fluvial aquifer materials (Fetter, 2001; Payne et al., 2008). Local variability will not have an impact on overall results, and 35% is a reliable estimate for the total porosity of the alluvium simulated in modeled layers 1 through 9.

With respect to the bedrock porosity, there is very low to negligible primary (intergranular) porosity but secondary porosity (bedrock fractures) is the main porosity associated with the bedrock. A dual domain model can be utilized to simulate flow through fractured bedrock. The basis for this approach is the fact that at large enough scale, fractured rock flow systems can be effectively simulated as porous media with low mobile porosity. As a general rule of thumb, the size of the block of fractured rock that may be treated as a porous media is often considered to be about 100 times the average fracture spacing (Gerber, Bither, and Muff, 1991). An analysis of the rock core logs from the Phase 1 and 2 ER-TCS area boreholes shows an average fracture spacing in the saturated zone to be about 0.29 feet. The transport model grid cell dimensions over the extent of the plume are 25 ft x 25 ft. The current model grid spacing is therefore close to the 100 times the fracture spacing, suggesting that it is reasonable to use the existing

model to simulate the fractured rock at Topock. The simulated total porosity to represent bedrock fracture flow (secondary porosity) was reduced to 2%, of which 1.9% simulated as mobile porosity and 0.1% as the immobile porosity.

4.2.2 Mass Transfer Coefficient

An estimated mass transfer coefficient (MTC) value of 1.0×10^{-3} /day was utilized for all model layers in the solute transport model. This MTC was developed based on a range of literature values and models of similar dimensions and aquifer properties (Gillham et al. 1984; Molz et al. 2006; Flach et al. 2004; Harvey and Gorelick, 2000; Feehley et al. 2000; Julian et al. 2001). The solute transport model was then run with initialized current plumes to determine if the selected MTC produced reasonable results with the constituent distribution currently observed. It was recognized that variations in historic plume interpretations were not just a function of plume movement, but also improved delineation of the plume that developed over time as the monitoring well network density evolved. The current plume interpretation is based on a much more advanced monitoring well network, which improved the resolution of the plume delineation. The MTC value for the solute transport model was systematically adjusted between 1.0×10^{-05} (1/day) and 1.0 (1/day), and small-scale and short-term plume movements were evaluated until the solute transport model produced reasonable plume movement.

4.2.3 Chromium Adsorption

The retardation factor (R_f) is used by the solute transport model to represent the amount of adsorption of a constituent from the dissolved or solute phase. The retardation factor used for Cr(VI) is based on the linear sorption isotherm and is calculated in MT3D using the bulk density (ρ_b), the porosity (n) of the aquifer material, and a distribution coefficient (K_d), according to the following equation:

$$R_f = 1 + \frac{\rho_b K_d}{n} \quad (4-1)$$

The presence of background Cr(VI) concentrations associated with the naturally occurring mineralogy suggests nominal adsorption (low K_d value) is representative of the aquifer. This assessment is consistent with the literature, which identifies a wide range of K_d values (USEPA 1999) for naturally occurring Cr(VI) in aquifer soils with a normal pH range. The calibration of the regional groundwater flow model to the growth of the Cr(VI) plume (CH2M Hill, 2005b) supports the limited retardation of Cr(VI) transport, and thereby low K_d values at the Site. If K_d values for Cr(VI) were larger, the extent of the Cr(VI) plume would be more limited than the current extents of the Cr(VI) plume footprint. Additionally, a laboratory study on aerobic core samples from the Site (CH2M Hill, 2005a) indicated the range in K_d values from two aerobic core samples collected from the flood plain varied between 0.01 and 0.09 L/kg. The model includes a small amount of adsorption for Cr(VI), incorporating a distribution coefficient (K_d) of 0.05 liter per kilogram (L/kg) in the aquifer, which falls within the range of reported K_d values. A K_d value of 0.05 L/kg in the aquifer results in a retardation factor of approximately 1.25 for the Cr(VI) plume in the solute transport model. This indicates the plume will migrate about 25% slower than the ambient groundwater flow velocity. Given the limits of the current plume and the understanding of groundwater flow through the region, the K_d value of 0.05 L/kg in the aquifer is a reasonable estimate of natural chromium adsorption rates at the Site. The Cr(VI) K_d value was further adjusted in the bedrock to better simulate the movement of Cr(VI) in the fractured bedrock. The bedrock was simulated with a total porosity of 2% so

the K_d value in bedrock was reduced to 0.0029 L/kg to yield an equivalent R_f as calculated in the aquifer to establish a uniform R_f value of 1.25 throughout the entire model domain.

4.2.4 Chromium Reduction

The reduction and precipitation of Cr(VI) in the aquifer was simulated by accounting for the reduction/precipitation of chromium in the presence of injected carbon (as part of an in-situ remediation approach). To account for this, the model utilized a Cr(VI) reduction/precipitation whenever the injected carbon exceeds a concentration of 0.1 mg/L. At the same time, a carbon half-life of 20 days was assigned to account for the degradation of the injected carbon over time. By simulating both Cr(VI) and carbon simultaneously, the interactions between the plume and the active IRZ were accounted for in the solute transport model.

4.2.5 Initial Hexavalent Chromium Distribution

The initial hexavalent chromium plume concentration distribution was based on all hexavalent chromium data collected through December 31, 2013. In the upper five model layers, the plume delineation varied to reflect the differing Cr(VI) concentrations encountered with depth. Cr(VI) was not initialized in model layers 6 through 10. The initialized Cr(VI) distributions are the same in both the mobile and immobile portions of the aquifer. The distribution of the Cr(VI) for model layers 1 through 5 are shown on Figure 4.2-1. Hexavalent chromium was also initialized for December 2015. The distribution of Cr(VI) for December 2015 for model layers 1 through 5 are shown on Figure 4.2-2.

4.2.6 Byproduct Generation

As discussed previously, the introduction of dissolved organic carbon into the aquifer will facilitate treatment of Cr(VI) in groundwater through precipitation of stable, low-solubility Cr(III) minerals. This precipitation reaction results from the formation of geochemical conditions that are similar to those currently present in the fluvial aquifer that comprises the rind adjacent to the river. Naturally occurring minerals in the rind are currently dissolved due to the presence of natural organic carbon, at the same time that Cr(VI) is undergoing precipitation in this rind. The goals of the in-situ groundwater treatment are to promote these geochemical conditions in order to facilitate treatment. Once geochemical conditions form in the alluvial aquifer that are similar to the fluvial aquifer, there will be natural minerals that dissolve (specifically natural iron minerals), and naturally occurring manganese and arsenic associated with these natural minerals may become soluble. These byproducts of the introduction of organic carbon will be generated only in the presence of organic carbon, and their migration will be limited in distance outside of the reactive zone where Cr(VI) is treated. These secondary water quality effects are discussed in detail in Appendix G of the CMS/FS (CH2M HILL, 2009b). Byproducts will be generated due to dissolution of naturally occurring iron minerals in the aquifer, and the distance over which they travel will be controlled by attenuation mechanisms, principally sorption. The solute transport model was used to evaluate the generation of byproducts and their fate and transport.

Byproduct generation is simulated in the fate and transport model by linking the concentration of organic carbon to a corresponding concentration of dissolved manganese and arsenic. Based on the floodplain and upland ISPT results (Arcadis 2008, 2009), the generation coefficients for manganese and arsenic were determined to be 0.016 mg of manganese per mg of organic carbon and 0.000108 mg of arsenic

per mg of organic carbon, respectively. A range of generation coefficients for manganese and arsenic were selected based upon this base case, as detailed in Table 4.2-1.

Table 4.2-1

Byproduct Generation Terms Used in Fate and Transport Model

Byproduct	Generation Term (mg of Byproduct per mg Organic Carbon per Liter)		
	Low	Base Case	High
Manganese	0.005	0.016	0.05
Arsenic	0.00005	0.000108	0.00018

4.2.7 Byproduct Adsorption and Precipitation

The dissolution of iron, manganese, and arsenic in the IRZs is temporary and these elements will then return to baseline concentrations. Iron, manganese, and arsenic that have dissolved and moved out of the reactive zone under the influence of groundwater flow will undergo reactions that will transition these dissolved, naturally occurring elements to sorbed or precipitated forms, thereby removing them from groundwater. Dissolved iron will react by sorbing to solid-phase iron minerals outside of the reactive zone, and it will also precipitate through reaction with dissolved oxygen in the aquifer. Manganese concentrations will attenuate via sorption, reoxidation, and precipitation reactions; and arsenic concentrations will attenuate via coprecipitation and sorption as described in Appendix B of the 100% Basis of Design (Arcadis, 2015). Oxygen will be introduced through the natural flux of dissolved oxygen in groundwater flowing from areas outside of the IRZ and from the river. In more oxic portions of the aquifer, Fe(II) uptake will occur both through reaction with dissolved oxygen and by adsorption to/oxidation by Fe(III) minerals, forming mixed Fe(II)/ (III)-oxides. Dissolved oxygen and iron minerals in the deeper aquifer will mix and come into contact with groundwater coming in from upgradient. As iron minerals accumulate downgradient of the IRZ, this will continue to provide additional sorption capacity for manganese and arsenic. This process of attenuation of iron by sorption, rather than re-oxidation, is similar to the attenuation mechanism that is anticipated and that was modeled for manganese as described in Appendix B of the 100% Basis of Design (Arcadis, 2015). Concentrations of these analytes will be monitored downgradient of the IRZ, and program modifications will be made as necessary if analyte concentrations exceed anticipated levels, as described in the Operations and Maintenance Manual Volume 2: Sampling and Analysis Plan (Appendix L of the 100% Basis of Design).

Changes in pH and production of dissolved gases are not anticipated to be a concern based on the in-situ pilot test (ISPT) results as well as results observed at Hinkley and other Sites. During pilot testing, no significant changes in pH were observed in monitoring wells, indicating that any pH changes caused by

DEVELOPMENT OF GROUNDWATER FLOW AND SOLUTE TRANSPORT MODELS

carbon consumption and subsequent redox/precipitation/dissolution reactions were adequately buffered by the aquifer solids.

Dissolved gas concentrations generated within the IRZ are anticipated to be sufficiently low as to minimize formation of a gas phase within the aquifer. Given the relatively low carbon concentration used in pilot testing and specified in the design, any CO₂ generated will be at a low enough concentration that it will remain dissolved and be flushed through the IRZ over time. Further, pH buffering to circumneutral values by the aquifer solids will ensure that most of the inorganic carbon generated will be present as bicarbonate rather than dissolved CO₂. Formation of H₂(g), H₂S, and methane will be limited by controlling TOC concentrations to limit byproduct generation. Formation of these gases (as well as N₂ formation) was not an issue during the pilot testing conducted in the floodplain. Gas generation was higher during the upland ISPT in locations where organic carbon was distributed at concentrations in the 5,000 to 10,000 mg/L TOC range. The upland ISPT results indicate that lower concentrations of organic carbon, which have been proven effective, should be used to prevent excess gas generation; and lower concentrations have been specified in the design. The changes associated with the in-situ system are not expected to affect the reducing rind enveloping the river. Downgradient of the IRZ within the floodplain, manganese attenuation is modeled via adsorption, whereas arsenic attenuation is modeled via rate-limited co-precipitation according to a given half-life. These processes are assumed not to occur within the IRZ itself, instead taking effect within the redox recovery zone downgradient of the IRZ. In the solute transport model, this process is captured by activating the manganese and arsenic attenuation mechanisms outside of the maximum simulated 1 mg/L TOC footprint.

Oxidation of Mn(II) was incorporated into the solute transport model by assuming a half-life of 29 days, and coprecipitation of arsenic was accounted for by assigning a half-life of 30 days (base case) derived from the ISPT data.

A summary of the sorption parameters used in the model is provided in Table 4.2-2, below. Development of these parameters is discussed in the 100% Basis of Design Sections 5.3.2 (for manganese) and 5.4.3 (for arsenic).

Table 4.2-2

Byproduct Sorption Terms Used in Fate and Transport Model

Byproduct	Freundlich Parameters		
	Low	Base Case	High
Manganese	$K_F=0.137, N=0.875$	$K_F=1.37, N=0.875$	$K_F=6.85, N=0.875$
Arsenic	$K_F=0.554, N=0.465$	$K_F=2.77, N=0.465$	$K_F=13.85, N=0.465$

4.3 Parameter Assessment

Future groundwater flow model calibrations during remedy installation and operation will utilize recent data sets along with historical calibration data sets to further calibrate the groundwater flow model. Upon completion of the calibration of the groundwater flow model, the solute transport model will be calibrated against recent concentration data and observed trends, in accordance with the schedule in Section 7. The solute transport model was adopted following the choice of remedy in the CMS, with the approved hydraulic model forming the basis of this model. A predictive sensitivity analysis was conducted in the 100% basis of design using the solute transport model by varying multiple solute transport model parameters and remedy operations, and observing the impact on Cr(VI), TOC, Mn, and As. Various aspects of the Cr(VI) plume and behavior of manganese and arsenic were analyzed in detail with the solute transport model to determine an appropriate range of solute transport parameters to use for the predictive modeling. Utilizing the data collected during installation and implementation of the remedy as described in Section 7 will also allow for further refinement of the model and the predicted performance of the remedy design can be further assessed.

4.4 Remediation Design

There are seven components of the remediation design that are simulated concurrently with the solute transport model to effectively remediate the hexavalent chromium plume while reducing the impact of potential byproducts:

- NTH IRZ (NTH IRZ Injection and Extraction Wells)
- River Bank extraction (River Bank Extraction Wells)
- Uplands injection (Inner Recirculation Loop [IRL] Injection Wells)
- Transwestern Bench extraction (Transwestern Bench Extraction Wells)
- East Ravine extraction (East Ravine Extraction Wells)
- TCS injection (TCS Injection Wells)
- Freshwater injection (Freshwater Injection Wells)

Details of each component is presented in the 100% Basis of Design Report (Arcadis, 2015). The remediation design is shown in Figure 4.4-1.

4.5 Pathline Analysis

Figures 4.5-1 to 4.5-10 show simulated groundwater pathlines under active remedy flow conditions in model layers 1 through 5, respectively. Each model layer has 2 figures to represent the different time periods with the NTH IRZ, active or inactive. These pathlines were delineated using MODPATH (Pollack, 1989). MODPATH is a program that is used in conjunction with MODFLOW to track the advective movement of groundwater and directly utilizes the computed flow information from the MODFLOW model. A ring of particles was initialized at each of the uplands injection, freshwater injection and TCS injection wells in each layer and run with forward particle tracking for a period of 30 years. These figures help to illustrate the movement of the injected water during the remedy operation and should not be used independently from the solute transport model in order to best evaluate remedy performance. For evaluation of hexavalent chromium, manganese and arsenic migration, the solute transport model is a more useful tool as it is able to account for mechanisms that would influence the behavior of these species in groundwater (i.e., sorption, reduction, oxidation, precipitation, etc.). For evaluation of TDS, these pathlines can be useful in helping to visualize the anticipated TDS footprint as the particles behave as a tracer without retardation. Focusing on the particles originating at injection wells IRL-1 and IRL-2, which receive River Bank extracted water in the nominal remediation operation scenario, indicates that these pathlines are encapsulated by the upgradient freshwater injection wells (IRL-3, IRL-4, and FW-1) thereby limiting the extent of potential elevated TDS concentrations associated with River Bank extracted water.

5 SOLUTE TRANSPORT MODEL RESULTS

5.1 Hexavalent Chromium

The solute transport model was run for a period of 30 years utilizing the transport parameters and flow conditions described in Section 4 for the simulated Cr(VI). The results are shown for years 0.5, 1.5, 3, 5, 10, 20, and 30 for each of the five model layers in which Cr(VI) was initialized on Figures 5.1-1 through 7.1-5. These figures show the impact the injected carbon concentrations and remediation design flow conditions are predicted to have on the chromium distribution over time. Carbon is actively injected into the NTH IRZ during the first 6 months of the simulation, followed by an 18-month period where the NTH IRZ is turned off. This 6-month on/18-month off NTH IRZ cycle period is repeated for the full duration of the transport run. This solute transport run indicates the NTH IRZ successfully creates a remediation barrier along the majority of the NTH IRZ line in all four model layers. The sections of the plume that are initialized on the east side of the NTH IRZ and the low Cr(VI) concentrations in the vicinity of the NTH IRZ wells that are not treated by the NTH IRZ (e.g., the low concentration finger of the plume that migrates past the northern NTH IRZ in model layers 3 and 4; see Figures 5.1-3 and 5.1-4, during the 18-month rest cycle when active pumping is suspended) are hydraulically controlled by the River Bank Extraction Wells. Most of the Cr(VI) remaining after 30 years of simulation is located in the bedrock in model layers 1 and 2 where the plume was initialized and persists due to the simulated low permeability of the bedrock. Due to the simulated low permeability of the bedrock, the sustainable yield in the bedrock is limited, so the East Ravine Extraction well rates were kept low. Based on the Cr(VI) transport results, minor modifications were made to operational rates in the NTH IRZ. NTH IRZ extraction well IRZ-5 was reduced by 20 gpm, and extraction well IRZ-9 was increased by 20 gpm in efforts to provide more control of the northern plume extents. As there is currently a limited monitoring well network in the northern portion of the plume,

there is uncertainty with the exact Cr(VI) plume distribution, but the plume was conservatively drawn to account for historic concentrations slightly greater than 32 ppb in the vicinity of IRZ-1. These adjusted rates fall within the range of remediation well design rates presented in Table 3.2-1 of the 100% Basis of Design (Arcadis, 2015).

The solute transport model was rerun with the 2015 Cr(VI) plumes initialized in model layers 1 through 5. The results are shown on Figures 5.1-6 through 5.1-10, respectively. There was no simulated hexavalent chromium present in model layers 6 through 10, so these layers were not presented. As there were only minor changes to the Cr(VI) plume distribution between 2013 and 2015, the 2015 Cr (VI) simulation results are similar to those with the 2013 initialized plume.

5.2 Manganese

Figure 5.2-1 shows the maximum manganese in all layers generated as a byproduct from the injection of carbon-amended groundwater for the 30-year simulation period. The manganese transport run indicates that portions of the naturally occurring manganese and generated manganese byproduct will be extracted by the River Bank Extraction Wells and injected into IRL-1 and IRL-2, located in the upland area. This potential manganese impact in the uplands needs to be monitored over time to avoid elevated manganese concentrations. A potential method to mitigate this upland manganese impact would be to reduce or terminate flow from the River Bank and/or blend the River Bank extracted water with the freshwater injection over the course of the remedial program. The simulated magnitude and extent of byproduct manganese using the revised groundwater flow model are generally consistent with simulated manganese in the 100% basis of design report.

5.3 Arsenic

Figure 5.3-1 shows the maximum simulated arsenic transport in all layers for the 30-year simulation period. The arsenic runs take into account both the simulated naturally occurring arsenic associated with the freshwater injection as well as potential arsenic generated as a byproduct from carbon amended injection wells. The solute transport run indicates that arsenic concentrations associated with carbon-amended injection never exceed 10 µg/L in the 30-year simulation period. The only arsenic concentrations that exceed 10 µg/L are associated with the naturally occurring arsenic concentrations that are injected into the 4 wells receiving freshwater injection at a concentration of 15 µg/L. Despite constant injection rates and arsenic concentrations at these locations, the expansion of the arsenic footprint is relatively slow. This is due to the fact that the simulated arsenic sorption regulates the extent of the injected arsenic distribution. The simulated magnitude and extent of freshwater arsenic and byproduct arsenic using the revised groundwater flow model are generally consistent with simulated manganese in the 100% basis of design report.

6 UNCERTAINTY

As with all mathematical models of natural systems, the groundwater flow and solute transport model is limited by factors, such as scale, accuracy of the estimated hydraulic properties and/or boundary conditions, and the underlying simplifications and assumptions incorporated into the model. These factors result in limitations to the model's appropriate uses and to the interpretations that may be made of the simulation results. The remedy design and range of operation were based on the conceptual Site model, calibrated groundwater flow model, the predictive solute transport modeling and sensitivity analysis, and professional judgment.

Several strategies were employed to address the uncertainties inherent to the predictive model. As discussed in Section 3, the flow model was calibrated against: (a) pre-IM-3 steady state conditions, (b) active IM-3 operating steady state conditions (2015), and (c) average monthly site conditions responding to fluctuating river levels and pumping during 2015. This calibration procedure utilized a stochastic approach that resulted in a highly heterogeneous distribution of hydraulic conductivity to represent the identified hydrostratigraphic units. Note that density-dependent flows (resulting from potential deviations in temperature and salinity) were not simulated because these will have a negligible impact on system flows and the remedy design when compared to the natural heterogeneity of the aquifer.

A dual domain mass-transfer approach was used to model solute transport in the heterogeneous aquifer system as the small-scale preferential flow pathways cannot be fully and explicitly represented by the spatial discretization in a numerical model for practical reasons. Uncertainty was further addressed by conducting a detailed sensitivity analysis on various hydraulic parameters. This sensitivity analysis can be utilized to identify the degree of sensitivity associated with each parameter.

With respect to TDS and density variations, while it is acknowledged that effects of density-driven flow may be possible, they are not expected to be significant. Given the aquifer heterogeneity and vertical anisotropy, and the relatively high expected flow velocities within the system in the vicinity to the freshwater injection wells, advection-driven flows are expected to allow adequate horizontal flows to develop and be maintained at all depths between freshwater injection wells and River Bank extraction wells. If however, effects of density are observed during remedy implementation (i.e. slower, or 'short-circuiting' of flushing within the deeper, more saline portions of the aquifer in areas some distance away from the injection wells with respect to monitored average hydraulic gradients), steps can be taken to mitigate these impacts. Potential steps include varying well flow rates over the entire screened zone, or packing off sections of upper screened intervals to increase flushing in deeper zones, effectively countering buoyant effects caused by density contrasts between injected freshwater and in-situ denser water.

7 MODEL UPDATE PROCEDURE

During remedy well installation and testing, after system start-up, and during remedy operation, data will be collected and analyzed to identify whether the groundwater flow, geochemical, and solute transport models differ from the conceptual Site model with respect to the hydrogeologic characterization or remedy performance. The groundwater flow model, geochemical model, and/or the solute transport model will be updated and recalibrated at the intervals defined in the sections below. This will allow the models to be used as predictive tools to evaluate remedy performance and assist in providing

DEVELOPMENT OF GROUNDWATER FLOW AND SOLUTE TRANSPORT MODELS

recommended optimizations for operation of the remedial system (i.e., injection/extraction rates and frequency, carbon dosing frequency and concentration, and need for provisional wells). The model can also be further utilized to support capture zone analyses by simulating the capture zones of extraction wells under operational conditions to supplement the other lines of evidence for hydraulic capture based on field data. This is critical where a limited monitoring network is present for the riverbank extraction wells due to their proximity to the Colorado River. The updated model will also be used to re-evaluate remediation timeframe estimates by integrating anticipated remedy component operational rates and carbon dosing frequency and concentration. The updates made to the model will be noted in the corresponding quarterly report and presented in detail in the annual report.

During each defined model update the following steps will be included:

- Hydraulic property distributions will be refined based on updates to the spatial distribution of aquifer test data and lithologic descriptions.
- Actual operational data will be integrated into the groundwater flow model (i.e. pumping rates, pumping schedule, and vertical flow distribution)
- The groundwater flow model will be recalibrated to average observed water levels during each model update interval.
- The groundwater flow model will be recalibrated to observed transient water levels to gauge hydraulic responses to pumping and/or river fluctuations where applicable.
- Geochemical modeling parameters will be refined based on observed water quality data and field parameters.
- Solute transport modeling parameters will be refined based on observed water quality data and field parameters as well as geochemical modeling.
- Actual remedy operation parameters will be integrated into the solute transport model (i.e. TOC concentration, TOC injection frequency, etc.).
- Solute transport model will be calibrated against observed movement of Cr(VI), Mn, and As during the previous time interval.
- After model calibration, predictive modeling runs will be conducted to evaluate the simulated remedy performance in the future.
- Potential design and operations updates will be considered to further optimize remedy operation (i.e. pumping rates, TOC dosing concentration, dosing and operational frequency)
- Assessment of hydraulic capture zones based on simulated capture delineation and hydraulic gradients.

7.1 Well Installation and Testing

During the remedy well construction and testing period, the geochemical, groundwater flow and solute transport models will be updated annually to evaluate potential impacts of data collected during construction on the planned remedy performance. This model update schedule will allow for data from

DEVELOPMENT OF GROUNDWATER FLOW AND SOLUTE TRANSPORT MODELS

multiple wells to be considered and integrated into the groundwater flow and solute transport model on a wider areal basis rather than on a well-by-well basis. Examples of how data collected during the well installation period will focus on specific hydrogeologic data and Cr(VI) data are described below:

- **Lithologic Descriptions:** Lithologic descriptions that are logged from each borehole based on the visual inspection of the retrieved core or the drill cuttings will be collected. Additional soil samples at select wells will be collected for analysis of physical properties. By comparing multiple borehole lithologic descriptions and available physical property data, local stratigraphy will be assessed to better identify any potential key continuous hydrogeologic features that can be incorporated into the groundwater flow model during the update and recalibration process.
- **Saturated Aquifer Thickness:** During well installation, the saturated aquifer thickness at each well will be determined by observing where both the water table and bedrock contact are encountered. This data can be utilized to refine the structure of the regional groundwater flow model and then be transferred into the model. The current model structure was interpolated from available monitoring well points and boring logs, and can be refined with additional data points to better represent the geologic structure. The new borehole/well information will be incorporated by first verifying the model structure in the area (alluvial aquifer and bedrock contact) and then aquifer properties gained from well testing will be assessed.
- **Hydraulic Conductivity/Transmissivity:** Constant rate and step rate aquifer tests will be conducted at select locations and the recorded data can be utilized to calculate approximate hydraulic conductivity / transmissivity data. The vertical and lateral distributions of hydraulic conductivity values will be used to guide hydraulic conductivity values during the calibration process. Depending on the distribution, hydraulic conductivity values may be averaged or used directly. The approximate spatial distribution of this data can be incorporated into the groundwater flow model during the model update and recalibration process. Any potential changes will be carried through in the model for future transport run simulations.
- **Hexavalent chromium distribution:** Groundwater samples will be collected and analyzed from the existing monitoring well network, as well as newly installed wells, during the well installation period. Cr(VI) data will be utilized to update the Cr(VI) plume distribution in the solute transport model for subsequent transport simulations to evaluate the remedy design. The vertical aquifer sampling (VAS) Cr(VI) data collected during well installation and testing will not be utilized to update the Cr(VI) plume distribution as this data is qualitative screening level data.

The data will be utilized to update and recalibrate the regional groundwater flow model. The groundwater flow model recalibration will involve adjustments to model parameters, structure, and boundary conditions as necessary to reduce the difference between the average observed and simulated water levels and hydraulic gradients. Groundwater flow model updates could include updates to the simulated geologic structure, hydraulic conductivity, and vertical hydraulic conductivity. The geochemical modeling parameters will be refined based on observed water quality data and field parameters. The solute transport model will be updated with the available hexavalent chromium data to reflect updated initial plume conditions and refined geochemical parameters will be integrated. The groundwater flow and solute transport model will then be utilized to rerun the initial baseline remedy to determine if there are changes in the simulated hexavalent chromium transport projections.

7.2 Remedy Start-up and Operation

Data collected during remedy start-up and operation will focus on injection and extraction rates, observed hydraulic responses (water levels, hydraulic gradients, and potentiometric surfaces), Cr(VI) concentrations, arsenic concentrations, manganese concentrations, and TOC distribution. Based on these data, the model will be updated to reflect the actual pumping rates attained during remedy start-up and the observed response in groundwater flow and solute transport. To evaluate remedy performance, the groundwater flow and solute transport model simulations will be compared against observed hydraulic and analytical data annually during the start-up period, as well as after each five years of remedy operation. The models will be updated according to this schedule so that the model can be further utilized as a predictive tool to evaluate remedy timeframes. By collecting the aforementioned data, the following are example parameters that can potentially be refined in the groundwater flow and solute transport models:

- **Operational Data:** Actual operational data will be integrated into the groundwater flow model (i.e., pumping rates, pumping schedule, and vertical flow distribution).
- **Hydraulic Conductivity / Transmissivity:** By evaluating the observed hydraulic responses during remedy operation the hydraulic conductivity / transmissivity parameters can potentially be refined. Comparing the simulated point water levels, potentiometric surfaces and hydraulic gradients to the observed field values, the regional groundwater flow model will be recalibrated under active remedy conditions. Upon completion of the groundwater flow model update, the solute transport model will be rerun to evaluate longer term remedy performance to evaluate the remedy timeframe.
- **Riverbed Conductance:** Although the riverbed conductance is not directly measured during remedy operation, this parameter will be evaluated during the calibration of the regional groundwater flow model. By monitoring the average groundwater level elevations under active remedy conditions, adjustments can potentially be made to the riverbed conductance to further improve the flow model calibration statistics.
- **Hexavalent Chromium Sorption:** The observed migration of hexavalent chromium based on the observed point data can be utilized to further determine if the simulated sorption parameters are still reasonable. This refinement will assist in assessing the overall plume velocity and associated remediation timeframe.
- **Hexavalent Chromium Distribution:** Based on the observed point hexavalent chromium concentrations, the hexavalent chromium plume distribution can be updated in each of the four model layers. This will assist in evaluating the performance of the remedy design and conduct long term model simulations to evaluate the predicted remedial timeframes.
- **TOC Degradation Rate:** The TOC concentrations will be observed to determine if the simulated degradation rate is appropriate or needs to be adjusted to reflect the developed reducing conditions downgradient from the NTH IRZ and the TCS injection wells. Adjusting this parameter will allow for refinement of the simulation of the extent, duration, and magnitude of the TOC in the simulated IRZ footprint.
- **Byproduct Generation:** The manganese and arsenic concentrations will be monitored downgradient of the active in-situ reactive wells to assess whether observed magnitudes and extents match

DEVELOPMENT OF GROUNDWATER FLOW AND SOLUTE TRANSPORT MODELS

modeled distributions. Adjustments can be made to the relationship between simulated TOC degradation and the mobilization of manganese and arsenic if observed data suggests modifications are needed.

- Byproduct Sorption: The byproduct manganese and arsenic Freundlich isotherm sorption parameters can be evaluated to compare field parameters to modeled parameters. These parameters will first be evaluated with the geochemical model and then transferred into the solute transport model. Predictive modeling can then be conducted.

The groundwater flow model will be recalibrated to average and transient observed water levels during each model update interval. Following groundwater flow model calibration, the assessment of hydraulic capture zones based on simulated capture delineation and hydraulic gradients will be conducted. Geochemical modeling parameters will be refined based on observed water quality data and field parameters. Solute transport modeling parameters will be refined based on observed water quality data and field parameters as well as geochemical modeling. The solute transport model will be calibrated against observed movement of Cr(VI), Mn, and As during previous time intervals. After model calibration, predictive modeling runs will be conducted to evaluate the simulated remedy performance in the future. Potential design updates and operations will be considered to further optimize remedy operation (i.e., pumping rates, TOC dosing concentration, dosing and operational frequency). The model will be used to predict future performance in conjunction with empirical data. The model will not be used for all changes associated with system operation where current empirical data is a more accurate reflection of system performance and the need for operational changes; such as flow rate changes, TOC feed adjustments, and maintenance needs.

8 SUMMARY AND CONCLUSIONS

The regional groundwater flow model was converted from MicroFEM to MODFLOW to develop a single tool to evaluate remedial design through both groundwater flow and solute transport. The model layer structure was revised to better account of the potential mass transfer between the groundwater in alluvium and bedrock. The major hydrostratigraphic units were defined using hydraulic conductivity zones throughout the revised model structure. The hydraulic conductivity zones were further manipulated by assigning a stochastic distribution to account for potential heterogeneities encountered in the aquifer. The model was calibrated to steady state conditions for both pre-IM-3 and active IM-3 operations, as well as a transient period for 1 year that simulated average monthly changes in river stage and pumping rates. Calibration results indicated the model was well calibrated. The calibrated groundwater flow model then underwent a series of sensitivity analyses to further evaluate the simulated hydraulic parameters.

The updated groundwater flow model was then utilized to examine the remedial design and solute transport modeling presented in the 100% basis of design report. Overall, the solute transport modeling conducted with the updated groundwater flow model results were similar to those of the 100% basis of design report. Hexavalent chromium footprints were similar over the simulated 30 year transport period with the exception of more persistent hexavalent chromium concentrations initialized in the bedrock due to the enhanced simulation of the alluvium/bedrock contact. Byproduct manganese and arsenic results were similar in extent and magnitude in the floodplain and downgradient of the TCS injection wells as

DEVELOPMENT OF GROUNDWATER FLOW AND SOLUTE TRANSPORT MODELS

those presented in the 100% basis of design. The simulated arsenic footprints associated with the freshwater injection into the upland wells also were similar in extent and magnitude as presented in the 100% basis of design report.

Based on this update of the groundwater flow model and associated solute transport modeling, the solute transport model results indicates that the planned remedy will be effective in remediating the current Cr(VI) plume distribution while minimizing the potential adverse impacts from byproduct generation. This updated groundwater flow model and solute transport model can be utilized as a tool to evaluate potential remedial options and supplements monitoring of the implemented remedial system to measure its effectiveness. During installation and implementation of the remedial system, the additional hydrogeologic and groundwater quality data generated can be utilized to update the groundwater flow and transport models to improve their effectiveness as tools for further understanding site conditions and optimizing the remedy performance.

9 REFERENCES

- Anderson, M. P. and W. W. Woessner. 1992. *Applied Groundwater Modeling: Simulation of Flow and Advective Transport*, Academic Press, Inc., New York, 381 p.
- Appelo, C.A.J., M.J.J. van der Weiden, C. Tournassat, and L. Charlet. 2002. Surface complexation of ferrous iron and carbonate on ferrihydrite and the mobilization of arsenic. *Environmental Science & Technology* 36: 3096-3103.
- Arcadis. 2008. Floodplain Reductive Zone In-Situ Pilot Test Final Completion Report. PG&E Topock Compressor Station, Needles, California. March 5, 2008.
- Arcadis. 2009. Upland Reductive Zone In-Situ Pilot Test Final Completion Report. PG&E Topock Compressor Station, Needles, California. March 3, 2009.
- Arcadis. 2009b. Third Quarter 2009 Monitoring Report for the Upland Reductive Zone In-Situ Pilot Test. PG&E Topock Compressor Station, Needles, California. December 15, 2009.
- Arcadis, 2015. 100% Basis of Design. PG&E Topock Compressor Station, Needles, California. November 2015.
- Banerjee, K., G.L. Amy, M. Prevost, S. Nour, M. Jekel, P.M. Gallagher, and C.D. Blumenschein. 2008. Kinetic and thermodynamic aspects of adsorption of arsenic onto granular ferric hydroxide (GFH). *Water Research* 42: 3371-3378.
- Burdige, D.J., S.P. Dhakar, and K.H. Nealson. 1992. Effects of manganese oxide mineralogy on microbial and chemical manganese reduction. *Geomicrobiology Journal* 10(1): 27-48.
- Burdige, D.J. 1993. The biogeochemistry of manganese and iron reduction in marine sediments. *Earth-Science Reviews* 35: 249-284.

DEVELOPMENT OF GROUNDWATER FLOW AND SOLUTE TRANSPORT MODELS

- CH2M HILL. 2010. Methods of Estimating Pore Volume Flushing Efficiency Used in Calculating Mass Removal Rates for CMS/FS Alternatives; Attachment A. PG&E Topock Compressor Station, Needles, California 2010.
- CH2M HILL. 2009a. RCRA Facility Investigation/Remedial Investigation Report, Volume 2: Hydrogeologic Characterization and Results of Groundwater and Surface Water Investigation. February 11, 2009.
- CH2M HILL. 2009b. Corrective Measures/Feasibility Study Report for Chromium in Groundwater, PG&E Topock Compressor Station, Needles, California. December 11, 2009.
- CH2M HILL. 2006a. Pore Water and Seepage Study Report, PG&E Topock Compressor Station, Needles, California. March 13, 2006.
- CH2M HILL. 2006b. Groundwater Model Report, Topock Compressor Station, Needles, California. June 2006.
- CH2M HILL. 2005a. Summary of Results—Aerobic Zone Hexavalent Chromium Core Testing, PG&E Topock Compressor Station, Needles, California. May 20, 2005.
- CH2M HILL. 2005b. Groundwater Model Update Report, PG&E Topock Compressor Station, Needles, California. July 29, 2005.
- Dixit, S. and Hering, J. 2003. Comparison of arsenic(V) and arsenic(III) sorption onto iron oxide minerals: Implications for arsenic mobility. *Environmental Science & Technology*, 37, 4182-4189.
- Dzombak, D.A., and Morel, F.M. 1990. *Surface Complexation Modeling: Hydrous Ferric Oxide*. New York: Wiley-Interscience. 393pp.
- Eary, L.E. and D. Rai. 1987. Kinetics of chromium (III) oxidation to chromium (VI) by reaction with manganese dioxide. *Environmental Science and Technology* 21: 1187-1193.
- Environment Agency UK. 2005. Groundwater-surface water interactions in the hyporheic zone. Science Report SC030155/SR1. Bristol: Environment Agency. 65 pp.
- Ecology and Environment (E&E). 2004. Draft RCRA Facility Investigation (RFI) Report, Bat Cave Wash Area, Pacific Gas and Electric Company's Topock Compressor Station. February.
- Essington, M.E. *Soil and Water Chemistry, An Integrative Approach*. New York: CRC Press. 534pp.
- Feehley, C.E., C. Zheng, and F.J. Molz. 2000. *A dual-domain mass transfer approach for modeling solute transport in heterogeneous aquifers: Application to the macrodispersion experiment (MADE) site*. *Water Resources Research* 36, no. 9: 2501–2515.
- Fetter, C.W. 2001. *Applied Hydrogeology Fourth Edition*. New Jersey: Prentice Hall, Inc.

DEVELOPMENT OF GROUNDWATER FLOW AND SOLUTE TRANSPORT MODELS

- Flach, G.P., S.A. Crisman, and F.J. Molz III, 2004. Comparison of Single-Domain and Dual-Domain Subsurface Transport Models. *Ground Water* 42, no. 6: 815-828.
- Fuller, C.C. and Harvery, J.W. 2000. *Reactive Uptake of Trace Metals in the Hyporheic Zone of a Mining-Contaminated Stream, Pinal Creek, Arizona*. *Environmental Science and Technology* 34(7): 1150-1155.
- Gandy, C.J., J.W.N. Smith, and A.P. Jarvis. 2006. Attenuation of mining-derived pollutants in the hyporheic zone: A review. *Science of the Total Environment*, 373(2-3), 435-446.
- Gerber, Bither, and Muff. 1991. *The Applicability of Porous Media Theory to Fractured Rock Flow in Maine*. Presented at National Water Well Association Regional Groundwater Conference (Eastern Focus Conference) in Portland Maine. October 29-31.
- Gillham, R.W., E.A. Sudicky, J.A. Cherry, and E.O. Frind. 1984. *An advection-diffusion concept for solute transport in heterogeneous unconsolidated geological deposits*. *Water Resources Research* 20, no.3: 369-378
- Gleyzes, C., Teller, S., Astruc, M. 2002. *Fractionation studies of trace elements in contaminated soils and sediments: a review of sequential extraction procedures*. *Trends in Analytical Chemistry* 21(6-7), 451-467.
- Guay, B.E. 2001. Preliminary Hydrologic Investigation of Topock Marsh, Arizona: 1995-98. PhD Dissertation, University of Arizona.
- Harvey, J.W., and Fuller, C.C. 1998. Effect of enhanced manganese oxidation in the hyporheic zone on basin-scale geochemical mass balance. *Water Resources Research*, 34(4), 623-636.
- Harvey, C.F., and S.M. Gorelick. 2000. *Rate-limited mass transfer or macrodispersion: Which dominates plume evolution at the macrodispersion experiment (MADE) site?* *Water Resources Research* 36, no. 3: 637-650.
- Hemker, C.J. 2006. MicroFEM, version 3.60. Groundwater flow modeling software, available at <http://www.microfem.com>.
- Howard, K. A., B.E. John, and J.E. Nielson. 1997. *Preliminary Geological Map of Eastern and Northern Parts of the Topock 7.5-minute Quadrangle, Arizona and California*, United States Geological Survey Open-File report 95-534
- Hunter, K.S., Y. Wang, and P. Van Cappellen. 1998. Kinetic modeling of microbially-driven redox chemistry of subsurface environments: coupling transport, microbial metabolism and geochemistry. *Journal of Hydrology* 209: 53-80.
- Hwang, I., B. Batchelor, M.A. Schlautman, and R. Wang. 2002. Effects of ferrous iron and molecular oxygen on chromium(VI) redox kinetics in the presence of aquifer solids. *Journal of Hazardous Materials* B92: 143-159.
- Julian, H.E., M.J. Boggs, C. Zheng, and C.E. Feehley. 2001. *Numerical simulation of a natural gradient tracer experiment for the natural attenuation study: Flow and physical transport*. *Ground Water* 39, no. 4: 534-545.

DEVELOPMENT OF GROUNDWATER FLOW AND SOLUTE TRANSPORT MODELS

- Kay, J.T., Conklin, M.H., Fuller, C.C., and O'Day, P.A. 2001. Processes of nickel and cobalt uptake by a manganese oxide forming sediment in Pinal Creek, Globe Mining District, Arizona. *Environmental Science & Technology*, 35(24), 4719-4725.
- Konikow, L. 1978. *Calibration of Groundwater Models, in Proceedings of the Specialty Conferences on Verification of Mathematical and Physical Models in Hydraulic Engineering*, College Park, Maryland, August 9-11, 1978.
- Kosmulski, M., S. Durand-Vidal, E. Maczka, and J.B. Rosenholm. 2004. Morphology of synthetic goethite particles. *Journal of Colloid and Interface Science* 271: 261-269.
- Manceau, A. 1995. The mechanism of anion adsorption on Fe oxides: Evidence for the bonding of arsenate tetrahedral on free Fe(O,OH)₆ edges. *Geochimica et Cosmochimica Acta*, 59: 3647-3653.
- Marble, J.C., Corley, T.L., Conklin, M.H., and Fuller, C.C. 1999. Environmental factors affecting oxidation of manganese in Pinal Creek, Arizona. U.S. Geological Survey Water-Resources Investigations Report 99-4018A, Volume 1, Section C.
- McDonald, M. G., and A. W. Harbaugh, 1988. *A Modular Three-Dimensional Finite-Difference Groundwater Flow Model, Techniques of Water-Resources Investigations, Book 6, Chapter A1*. U. S. Geological Survey. Reston, Virginia.
- Metzger, D.G., Loeltz, O.J. 1973. *Geohydrology of the Needles Area, Arizona, California, and Nevada*. U.S. Geological Professional Paper 486-J
- Molz, F.J., C. Zheng, S.M. Gorelick, and C.F. Harvey. 2006. *Comment on "Investigating the Macrodispersion Experiment (MADE) site in Columbus, Mississippi, using a three-dimensional inverse flow and transport model" by Heidi Christiansen Barlebo, Mary C. Hill, and Dan Rosbjerg*. *Water Resources Research*. 42 no. 6 W06603
- Morel, F.M.M. and J.G. Hering. 1993. *Principles and Applications of Aquatic Chemistry*. John Wiley & Sons, Inc., New York.
- Morgan, J.J. 2005. Kinetics of reaction between O₂ and Mn(II) species in aqueous solutions. *Geochimica et Cosmochimica Acta* 69(1): 35-48.
- Myers, C.R. and K.H. Nealson. 1988. Bacterial manganese reduction and growth with manganese oxide as the sole electron acceptor. *Science* 240: 1319-1321.
- Parkhurst, D., and C.A.J. Appelo. 1999. User's guide to PHREEQC (Version 2) – A computer program for speciation, batch-reaction, one-dimensional transport, and inverse geochemical calculations. U.S. Geological Survey Water Resources Investigations Report 99-4259.
- Payne, F.C., J.A. Quinnan, and S.T. Potter. 2008. *Remediation Hydraulics*. CRC Press, Boca Raton, Florida.
- Potter, S.T., Moreno-Barbero, E., and Divine, C.E. 2008. MODALL: A practical tool for designing and optimizing capture systems. *Ground Water*, 46(2): 335-340.

DEVELOPMENT OF GROUNDWATER FLOW AND SOLUTE TRANSPORT MODELS

- Pollock, D. 1989. Documentation of Computer Programs to Compute and Display Pathlines Using Results for the U.S. Geological Survey Modular Three-Dimensional Finite-Difference Ground-Water Flow Model. U.S. Geological Survey Open File Report 89-381. Reston, Virginia.
- Prommer, H., D.A. Barry, and C. Zheng. 2003. MODFLOW/MT3DMS based reactive multicomponent transport modeling. *Ground Water* 41(2): 247-257.
- Rai, D., D.A. Moore, N.J. Hess, L. Rao, and S.B. Clark. 2004. Chromium(III) hydroxide solubility in the aqueous $\text{Na}^+\text{-OH-H}_2\text{PO}_4\text{-HPO}_4^{2-}\text{-PO}_4^{3-}\text{-H}_2\text{O}$ system: A thermodynamic model. *Journal of Solution Chemistry* 33(10): 1213-1242.
- Robin, M.J.L., A.L. Gutjahr, E.A. Sudicky, and J.L. Wilson. 1993. Cross-Correlated Random Filed Generation with Direct Fourier Transform Method. *Water Resources Research*, 29(7): 2385-2397.
- Sass, B.M., and D. Rai. 1987. Solubility of amorphous chromium(III)-iron(III) hydroxide solid solutions. *Inorganic Chemistry* 26: 2228-2232.
- Smedley, P.L., and Kinniburgh, D.G. 2002. A review of the source, behaviour and distribution of arsenic in natural waters. *Applied Geochemistry* 17: 517-568
- U.S. Environmental Protection Agency. 1999. Understanding Variation in Partition Coefficient, K_d , Values, Volume II: Review of Geochemistry and Available K_d Values for Cadmium, Cesium, Chromium, Lead, Plutonium, Radon, Strontium, Thorium, Tritium, and Uranium. Appendix E.
- U.S. Geological Survey 1999. Parkhurst, D.L. and Appelo, C.A.J. User's Guide to PHREEQC (Version 2) – A Computer Program for Speciation, Batch-Reaction, One-Dimensional Transport, and Inverse Geochemical Calculations. United States Geological Survey Water-Resources Investigations Report 99-4259.
- Van Geen, A., A.P. Robertson, and J.O. Leckie. 1994. Complexation of carbonate species at the goethite surface: Implications for adsorption of metal ions in natural waters. *Geochimica et Cosmochimica Acta*, 58: 2073-2086.
- Ward, J.D., C.T. Simmons, and P.J. Dillon. 2008. Variable-density modelling of multiple-cycle aquifer storage and recovery (ASR): importance of anisotropy and layered heterogeneity in brackish aquifers. *Journal of Hydrology* 356(1-2): 93-105.
- Zheng, C. 1990. *MT3D: A Modular Three-Dimensional Transport Model for Simulation of Advection, Dispersion, and Chemical Reactions of Contaminants in Groundwater Systems*. Prepared for the U.S. Environmental Protection Agency. Robert S. Kerr Environmental Research Laboratory, Ada, Oklahoma. Developed by S.S. Papadopoulos & Associates, Inc., Rockville, Maryland.
- Zheng, C., and G. D. Bennett. 2002. *Applied Contaminant Transport Modeling Second Edition*, John Wiley & Sons, New York, 621 pp.
- Zheng, C., and P. Wang. 1999. *MT3DMS: A Modular Three-Dimensional Multispecies Transport Model for Simulation of Advection, Dispersion, and Chemical Reactions of Contaminants in Groundwater Systems*. Prepared for the U.S. Army Corps of Engineers, Washington, DC. University of Alabama, Tuscaloosa.

DEVELOPMENT OF GROUNDWATER FLOW AND SOLUTE TRANSPORT MODELS

TABLES



FIGURES



APPENDIX A

Transient Calibration Data



Arcadis U.S., Inc.

10 Friends Lane

Suite 200

Newtown, Pennsylvania 18940

Tel 267 685 1800

Fax 267 685 1801

www.arcadis.com